ORIGINAL PAPER

Fully distributed control for task-space formation tracking of nonlinear heterogeneous robotic systems

Xiang-Yu Yao · Hua-Feng Ding · Ming-Feng Ge

Abstract This paper studies task-space formation tracking problem of nonlinear heterogeneous robotic systems involving external disturbances, kinematic and dynamic uncertainties, where the cases with both single and multiple time-varying leaders are considered. To solve the aforementioned nonlinear control problem, several novel fully distributed control algorithms, in which no global information is employed, are developed for the nonlinear systems under directed communication topologies. Based on the proposed control algorithms, the control process is classified into two parts, namely the task-space formation tracking of master robots with a single leader and that of slave robots with multiple leaders. By invoking Barbalat's lemma and input-to-state stability theory, the sufficient criteria for the asymptotic convergence of the task-space formation tracking errors are established. In addition, the obtained results are extended to formation-containment and consensus problems in similar nonlinear cases. Finally, numerical examples are provided to illustrate the validity and advantages of the main results.

X.-Y. Yao · H.-F. Ding (✉) · M.-F. Ge (✉)
School of Mechanical Engineering and Electronic
Information, China University of Geosciences,
Wuhan 430074, China
e-mail: dinghf@cug.edu.cn

M.-F. Ge
e-mail: fmgabc@163.com

1 Introduction

Distributed control of multiple robotic systems (MRSs) has attracted large amount of attention in the control field, due to its major advantages including high adaptivity, strong robustness, low cost, flexible maneuverability and the extensive potential applications, for instance, cooperative formation tracking, collaborative localization, surveillance and monitoring, teleoperation, to name just a few, see [1–13] and the references therein.

Among the aforementioned applications of distributed control technologies, formation tracking control is one of the most hot topics, which aims to steer a cluster of robots to shape prescribed geometric patterns and track reference leaders under different kinds of communication topologies. A common and effective strategy used to address the control problem is the leader–follower-based control algorithm, which has been developed and investigated intensively from various perspectives. For instance, reference [14] has proposed an adaptive control algorithm for single-master multi-slave robotic systems, where the slave robots cooperatively construct a dynamic formation to handle one object under a single leader. Yu et al. [15] have investigated the formation tracking of

nonholonomic vehicles, where the vehicles maintain a desired formation and move along a static circle with a given static leader. In [16], three adaptive control strategies have been proposed for homogeneous networked nonlinear systems to achieve desired joint-space formation and track a moving leader with uncertain dynamics. The authors in [17,18] have studied the formation tracking of a group of nonlinear mechanical systems with uncertain dynamics and a virtual leader by designing distributed formation learning control schemes. However, the aforementioned literature mainly focuses on joint-space control of nonlinear homogeneous robotic systems with a single leader, which may restrict its applications if the single leader is disabled in some cases. Besides, the previous work on the formation tracking problem discussed in [19–21] focuses on linear, second- or higher-order nonlinear homogeneous dynamics, and the external disturbances, kinematic and dynamic uncertainties are not considered completely. Thus, it naturally motivates a challenging research topic focusing on formation tracking problems with multiple time-varying leaders, especially for the task-space formation of NHRSs with external disturbances, kinematic and dynamic uncertainties.

Additionally, another hot topic is fully distributed control, where the control algorithms are designed without using any global information. To deal with formation tracking of MRSs with a leader, fully distributed learning schemes have been proposed in [16] by designing adaptive controllers. To cope with the leader–follower consensus of linear MRSs, a fully distributed consensus protocol has been developed in [22] under directed communication topologies and a single leader. To solve consensus tracking of MRSs with uncertain dynamics, fully distributed adaptive laws have been adopted in [23] to track an active leader under directed and connected topologies. To handle the synchronization of MRSs following a dynamic leader, some fully distributed coupling laws have been proposed in [24] under undirected networks. To address optimization output regulation problems with unknown dynamics and an external leader, a fully distributed law driven by estimated regulation errors has been presented in [25]. Likewise, the above fully distributed control algorithms are designed for joint-space control of linear or homogeneous systems with a single leader, which do not completely consider the external disturbances, kinematic and dynamic uncertainties, and

cannot deal with the control problem in the case of leader failure. Moreover, note that the fully distributed adaptive laws presented in [24–27] are designed based on undirected or strongly connected communication topologies, which are only special cases of the spanning tree. It thus motivates us to investigate the task-space fully distributed formation tracking control problem for NHRSs with external disturbances, kinematic and dynamic uncertainties under generally directed topologies and multiple time-varying leaders.

Motivated by the above discussion, this paper investigates the task-space formation tacking of NHRSs in a fully distributed manner. The main contributions are summarized as follows. (1) In contrast to the control of linear or homogeneous systems without disturbances and uncertain parameters [19,22,25], this paper studies the NHRSs with external disturbances, kinematic and dynamic uncertainties. (2) Comparing with the joint-space formation control problem with a single leader [16–18], this paper employs NHRSs to realize two classes of task-space formation with both single and multiple time-varying leaders, respectively, which enriches the scenarios of coordination behaviors. (3) Superior to our previous results [10,11], the control algorithms developed for NHRSs are conceived in a fully distributed manner by employing sliding-mode gain and disturbance observer under generalized directed communication topologies.

The reminder of the paper is arranged as follows. The system formulation and problem description are presented in Sect. 2. Task-space formation tracking control algorithms and main results are given in Sect. 3. Numerical examples are provided in Sect. 4. The conclusions and prospects are proposed in Sect. 5.

Notations Throughout this paper, $\mathbb{R}^p$ and $\mathbb{R}^{d \times p}$ are, respectively, the $p \times 1$ and $d \times p$ real matrices. A^T and A^{-1} are the transposed and inverse matrix of matrix A, respectively. $\lambda_{\min}(A)$ stands for the minimum eigenvalue of matrix A, and I_n is the $n \times n$ identity matrix. $\max(x, y)$ denotes the maximum among the values. $\|z\|$ is the Euclidean norm, with supremum described by $\sup \|z\|$. and $\otimes$ is the Kronecker product. $a = [a_1; \ldots; a_n]$ denotes a column vector, while $b = [b_1, \ldots, b_n]$ denotes a row vector.

2 System formulation and problem description

2.1 System formulation

A robot, with joint- and task-space coordinates, respectively, described with $q \in \mathbb{R}^p$, $x \in \mathbb{R}^d$, is nonredundant if $p = d$ and redundant if $p > d$. Thus, for a NHRS, with numerous nonredundant and redundant robots, the kinematics and dynamics of the ith robot can be described by [28,29]:

$$x_i = \hbar_i(q_i), \quad \dot{x}_i = J_i(q_i)\dot{q}_i, \tag{1a}$$

$$H_i(q_i)\ddot{q}_i + C_i(q_i, \dot{q}_i)\dot{q}_i + g_i(q_i) = u_i + \mu_i, \tag{1b}$$

where $\hbar : \mathbb{R}^{p_i} \to \mathbb{R}^{d_i}$ maps the joint position states to task coordinates, $\dot{x}_i \in \mathbb{R}^{d_i}$ is the task-space velocity; $J_i(q_i) = \partial \hbar_i(q_i)/\partial q_i \in \mathbb{R}^{d_i \times p_i}$ is the Jacobian matrix assumed to be nonsingular; $H_i(q_i) \in \mathbb{R}^{p_i \times p_i}$ is the positive-definite inertia matrix and $C_i(q_i, \dot{q}_i) \in \mathbb{R}^{p_i \times p_i}$ is the Coriolis–centrifugal matrix; $g_i(q_i), u_i, \mu_i \in \mathbb{R}^{p_i}$ are, respectively, the vectors of gravitational force, control input and external disturbance applied at joints. Throughout this paper, kinematics (1a) and dynamics (1b) satisfy the following common properties [28–30].

Property 1 *If vectors $y \in \mathbb{R}^{p_i}$ is differentiable, kinematics (1a) can be linearized as*

$$J_i(q_i)y = Y_{ki}(q_i, y)\vartheta_{ki}, \tag{2}$$

where $Y_{ki}(q_i, z)$ and ϑ_{ki} denote a kinematic regressor matrix and a constant vector, respectively, while, in practical cases where the mass, moment of inertia and orientation of the objects are unknown, i.e., (2) with kinematic uncertainties $\hat{\vartheta}_{ki}$, thus one obtains

$$\hat{J}_i(q_i)y = Y_{ki}(q_i, y)\hat{\vartheta}_{ki}, \tag{3}$$

where $\hat{J}_i(q_i)$ and $\hat{\vartheta}_{ki}$ are estimators of $J_i(q_i)$ and ϑ_{ki}, respectively.

Property 2 *The matrices $\dot{H}_i(q_i)$ and $\frac{1}{2}\dot{H}_i(q_i) - C_i(q_i, \dot{q}_i)$ are symmetric and skew-symmetric, respectively. Thus there exists a vector $z \in \mathbb{R}^{p_i}$ satisfying $z^\mathrm{T}\left(\frac{1}{2}\dot{H}_i(q_i) - C_i(q_i, \dot{q}_i)\right)z = 0$.*

Property 3 *The dynamic parameters $H_i(q_i)$, $C_i(q_i, \dot{q}_i)$ and $g_i(q_i)$ are all bounded.*

Property 4 *If vectors $y, z \in \mathbb{R}^{p_i}$ are differentiable, dynamics (1b) can be linearized as*

$$H_i(q_i)y + C_i(q_i, \dot{q}_i)z + g_i(q_i)$$
$$= Y_{di}(q_i, \dot{q}_i, y, z)\vartheta_{di}, \tag{4}$$

where $Y_{di}(q_i, \dot{q}_i, y, z)$ and ϑ_{di} denote a dynamic regressor matrix and a constant vector, respectively. For the details of linearization process, please see the hereafter examples. Likewise, if dynamic uncertainty $\hat{\vartheta}_{di}$ is contained in (4), one obtains

$$\hat{H}_i(q_i)y + \hat{C}_i(q_i, \dot{q}_i)z + \hat{g}_i(q_i)$$
$$= Y_{di}(q_i, \dot{q}_i, y, z)\hat{\vartheta}_{di}, \tag{5}$$

where $\hat{H}_i(q_i)$, $\hat{C}_i(q_i, \dot{q}_i)$, $\hat{g}_i(q_i)$, $\hat{\vartheta}_{di}$ are estimators of $H_i(q_i)$, $C_i(q_i, \dot{q}_i)$, $g_i(q_i)$, ϑ_{di}, respectively.

Remark 1 For simplicity, all the robots are assumed to have identical task-space degrees of freedom such that all d_i can be abbreviated as d. Moreover, by invoking kinematic and dynamic uncertainties $\hat{\vartheta}_{ki}$ and $\hat{\vartheta}_{di}$, system (1) becomes a more suitable representation of practical robotic or mechanical system, which can improve its feasibility and robustness.

2.2 Graph theory and problem description

In order to describe the communications of the robots in NHRS, this paper employs a directed graph $\mathcal{G} = \{\mathcal{V}, \mathcal{E}, \mathcal{A}\}$, where $\mathcal{V}, \mathcal{E} \subseteq \mathcal{V} \times \mathcal{V}$ and $\mathcal{A} = [\omega_{ij}]$, respectively, denote the node set, the edge set and the adjacency matrix. Define the neighbors of node i be $\mathcal{N}_i = \{j \in \mathcal{V} \mid (j, i) \in \mathcal{E}\}$, where $(j, i) \in \mathcal{E}$ is the information transmitted from node j to node i. Thereafter, it gives $\omega_{ij} > 0$ if $j \in \mathcal{N}_i$, and $\omega_{ij} = 0$ otherwise. Meanwhile, set $\omega_{ii} = 0$ for any self-edge in this paper. Additionally, the corresponding Laplacian matrix $\mathcal{L} = [l_{ij}]$ is defined as $l_{ij} = \sum_{j \in \mathcal{N}_i} \omega_{ij}$ for $i = j$, and $l_{ij} = -\omega_{ij}$ for $i \neq j$. For a directed graph, one says there exists a directed spanning tree if a neighborless root node exists and has directed paths to all the other nodes. More details about basic concepts of graph theory can refer to [31,32].

Assumption 1 For the convenience of later reference, suppose there exist m master robots and $n - m$ slave robots in NHRS, denoted by the vectors $\mathrm{X}_m = [x_1; x_2; \ldots; x_m]$ and $\mathrm{X}_s = [x_{m+1}; x_{m+2}; \ldots; x_n]$, respectively. Moreover, a known virtual leader $x_0 \in \mathbb{R}^d$, defined as the neighborless root node, is assumed to be available to all the master robots, with the weight vector given as $\mathcal{B} = [b_1; \ldots; b_m]$.

Remark 2 With the introduction of the virtual leader, master and slave robots in Assumption 1, two predefined configurations, namely the formation tracking

of master robots with a single leader (*i.e.*, the virtual leader) and that of slave robots with multiple leaders (*i.e.*, the master robots), will be constructed. Moreover, in order to enhance the reliability of the later formation in the event of leaders failure, we suppose that the information of the virtual leader can always be available to all the master robots even if the virtual leader is disabled.

Assumption 2 The directed graph $\mathcal{G}$ contains at least a directed spanning tree, for example, information can always be successfully transmitted along directed paths from the master robots to all the slave robots, including the case that information transmitted among the slave robots.

Lemma 1 ([30]) *Based on Assumptions 1 and 2, the Laplacian matrix $\mathcal{L}$ corresponding to graph $\mathcal{G}$ can be written as the form*

$$\mathcal{L} = \begin{bmatrix} L_1 & 0 \\ L_2 & L_3 \end{bmatrix}, \tag{6}$$

where $\mathcal{L} \in \mathbb{R}^{n \times n}$, $L_1 \in \mathbb{R}^{m \times m}$, $L_2 \in \mathbb{R}^{(n-m) \times m}$. Note that $L_3 \in \mathbb{R}^{(n-m) \times (n-m)}$ is invertible, and $-L_3^{-1} L_2$ is nonnegative, with each row summing equal to one.

Proof See "Appendix A."   □

Definition 1 With the guidance of the virtual leader, the task-space formation tracking with a single leader is said to be achieved if there exists vector $\delta_i \in \mathbb{R}^d$ satisfying

$$\begin{aligned} &\lim_{t \to \infty} (x_i(t) - \delta_i - x_0(t)) = 0, \\ &\lim_{t \to \infty} (\dot{x}_i(t) - \dot{x}_0(t)) = 0, \end{aligned} \tag{7}$$

where $i \in \{1, \ldots, m\}$, δ_i is the constant position offset with respect to that of the virtual leader.

Definition 2 With the guidance of the master robots, the task-space formation tracking with multiple leaders is said to be achieved if there exist positive constants γ_j satisfying $\sum_{j=1}^m \gamma_j = 1$ and vector $\eta_i \in \mathbb{R}^d$ such that

$$\begin{aligned} &\lim_{t \to \infty} \left(x_i(t) - \eta_i - \sum_{j=1}^m \gamma_j x_j(t) \right) = 0, \\ &\lim_{t \to \infty} \left(\dot{x}_i(t) - \sum_{j=1}^m \gamma_j \dot{x}_j(t) \right) = 0, \end{aligned} \tag{8}$$

where $i \in \{m + 1, \ldots, n\}$, η_i is the constant position offset with respect to the convex of the master robots.

Remark 3 Hereafter, the time index t is omitted in expressions of x_i, x_j and other variables for the conciseness of mathematical representations. By solving the problem in Definitions 1 and 2, the obtained results can be extended to achieve multiple tasks involving formation, containment, flocking and consensus, simultaneously.

For convenience of later convergence analysis, the following Barbalat's lemma and input-to-state stability theory are introduced to obtain asymptotically stable systems.

Lemma 2 (Barbalat's lemma [33]) *If the system $x = f(t)$ is twice differentiable, $\dot{f}(t) \in \mathcal{L}_\infty$ and $\ddot{f}(t) \in \mathcal{L}_\infty$, respectively, indicate that $f(t)$ and $\dot{f}(t)$ are uniformly continuous. Moreover, if $f(t) \in \mathcal{L}_p (1 \le p \le \infty)$, and (i) $f(t)$ is uniformly continuous, then $f(t) \to 0$ as $t \to \infty$; (ii) $\dot{f}(t)$ is uniformly continuous, then $\dot{f}(t) \to 0$ as $t \to \infty$.*

Lemma 3 (Input-to-state stability theory [34]). *Assume a continuously differentiable system $\dot{z} = f(t, z, \tau)$, with globally Lipschitz for (z, τ) and uniformly in t. If the unforced system $\dot{z} = f(t, z, 0)$ has a globally exponentially stable equilibrium point at the origin $z = 0$, then it is input-to-state stable.*

3 Task-space formation tracking of NHRS

In this section, novel fully distributed algorithms are developed for NHRS to realize the formation tracking problem presented in Definitions 1 and 2, *i.e.*, $x_i - \delta_i - x_0$, $\dot{x}_i - \dot{x}_0 \to 0$ for $i \in \{1, \ldots, m\}$, and $x_i - \eta_i - \sum_{j=1}^m \gamma_j x_j$, $\dot{x}_i - \sum_{j=1}^m \gamma_j \dot{x}_j \to 0$ for $i \in \{m + 1, \ldots, n\}$ as $t \to \infty$.

3.1 Task-space formation tracking with a single leader

For the first part, the task-space formation tracking of master robots with a single leader is considered. For obtaining a fully distributed control algorithm, the estimators $\hat{x}_i, \dot{\hat{x}}_i, \ddot{\hat{x}}_i \in \mathbb{R}^d$ are firstly defined as

$$\begin{aligned} \dot{\hat{x}}_i &= -\beta_{1i} \text{sgn}(\sigma_i), \\ \ddot{\hat{x}}_i &= -\beta_{2i} \text{sgn}(\dot{\sigma}_i), \\ \dddot{\hat{x}}_i &= -\beta_{3i} \text{sgn}(\ddot{\sigma}_i), \end{aligned} \tag{9}$$

where $i \in \{1, \ldots, m\}$, $\sigma_i = \sum_{j=1}^m \omega_{ij}(\hat{x}_i - \hat{x}_j - \delta_i + \delta_j) + b_i(\hat{x}_i - \delta_i - x_0)$, $\hat{x}_i$ and $\hat{x}_j$ are the estimates of x_i and x_j; β_{1i}, β_{2i} and β_{3i} are three proper

time-varying coupling gains generated from the following adaption law.

$$\dot{\beta}_{1i} = \sigma_i^T \Gamma_{1i} \sigma_i,$$
$$\dot{\beta}_{2i} = \dot{\sigma}_i^T \Gamma_{2i} \dot{\sigma}_i, \tag{10}$$
$$\dot{\beta}_{3i} = \ddot{\sigma}_i^T \Gamma_{3i} \ddot{\sigma}_i,$$

Before providing main theorems, we would like to provide the following important result.

Theorem 1 *Consider the following closed-loop system under Assumptions* 1 *and* 2.

$$\dot{x}_i = -\beta_i \operatorname{sgn}\left(\sum_{j=1}^m \omega_{ij}(x_i - x_j) + b_i(x_i - x_0)\right), \tag{11a}$$

$$\dot{\beta}_i = \left(\sum_{j=1}^m \omega_{ij}(x_i - x_j) + b_i(x_i - x_0)\right)^T$$
$$\times \Gamma_i \left(\sum_{j=1}^m \omega_{ij}(x_i - x_j) + b_i(x_i - x_0)\right), \tag{11b}$$

then, one obtains $x_i - x_0 = 0$ *in finite time.*

Proof See "Appendix B." □

Based on Theorem 1, we discuss (9) and (10) with Assumptions 1 and 2, Then by a similar proof that performed in Theorem 1, one obtains $\sigma_i = 0$, $\dot{\sigma}_i = 0$, $\ddot{\sigma}_i = 0$ in finite time, namely the vector form $(L_1 \otimes I_d)(\hat{X}_m - \delta - (I_m \otimes x_0)) = 0$, $(L_1 \otimes I_d)(\dot{\hat{X}}_m - (I_m \otimes \dot{x}_0)) = 0$, $(L_1 \otimes I_d)(\ddot{\hat{X}}_m - (I_m \otimes \ddot{x}_0)) = 0$, where $\hat{X}_m = [\hat{x}_1; \ldots; \hat{x}_m]$, $\delta = [\delta_1; \ldots; \delta_m]$. Thus, it follows that $\hat{x}_i - \delta_i - x_0 = 0$, $\dot{\hat{x}}_i - \dot{x}_0 = 0$, $\ddot{\hat{x}}_i - \ddot{x}_0 = 0$ can be achieved in finite time, assumed as t_1.

Remark 4 By above discussion, one obtains $\hat{x}_i - \delta_i - x_0 = 0$, $\dot{\hat{x}}_i - \dot{x}_0 = 0$, $\ddot{\hat{x}}_i - \ddot{x}_0 = 0$ as $t > t_1$. Note that the most important is not the accurate value of the time t_1, but the results can be obtained in a finite time.

With the definition of the above sliding-mode estimators, a joint-space reference velocity $\dot{q}_{ri} \in \mathbb{R}^{p_i}$ is designed for master robot $i \in \{1, \ldots, m\}$ as follows.

$$\dot{q}_{ri} \triangleq \hat{J}_i^+ \left(\dot{\hat{x}}_i - \alpha_1 \tilde{x}_i\right) + \left(I_{p_i} - \hat{J}_i^+ \hat{J}_i\right) \lambda_i, \tag{12}$$

where $\hat{J}_i^+ = \hat{J}_i^T (\hat{J}_i \hat{J}_i^T)^{-1}$, especially $\hat{J}_i^+ = \hat{J}_i^{-1}$ for nonredundant robots, α_1 is a designed positive constant,

$\tilde{x}_i = x_i - \hat{x}_i$, and $\lambda_i \in \mathbb{R}^{p_i}$ is an optimized convex function for the master robots.

By (12), we get the following joint-space sliding vector $s_i \in \mathbb{R}^{p_i}$ and reference acceleration $\ddot{q}_{ri} \in \mathbb{R}^{p_i}$.

$$s_i \triangleq \dot{q}_i - \dot{q}_{ri}$$
$$\triangleq \dot{q}_i - \hat{J}_i^+ \left(\dot{\hat{x}}_i - \alpha_1 \tilde{x}_i\right) - \left(I_{p_i} - \hat{J}_i^+ \hat{J}_i\right) \lambda_i, \tag{13a}$$

$$\ddot{q}_{ri} \triangleq \dot{\hat{J}}_i^+ \left(\dot{\hat{x}}_i - \alpha_1 \tilde{x}_i\right) + \hat{J}_i^+ \left(\ddot{\hat{x}}_i - \alpha_1 \dot{\tilde{x}}_i\right)$$
$$+ \frac{d}{dt}\left(\left(I_{p_i} - \hat{J}_i^+ \hat{J}_i\right) \lambda_i\right), \tag{13b}$$

where $\dot{\hat{J}}_i^+ = \dot{\hat{J}}_i^T (\hat{J}_i \hat{J}_i^T)^{-1} - \hat{J}_i^T (\hat{J}_i \hat{J}_i^T)^{-1}(\dot{\hat{J}}_i \hat{J}_i^T + \hat{J}_i \dot{\hat{J}}_i^T)(\hat{J}_i \hat{J}_i^T)^{-1}$, especially $\dot{\hat{J}}_i^+ = -\hat{J}_i^{-1} \dot{\hat{J}}_i \hat{J}_i^{-1}$ for nonredundant robots.

Then, the control input, kinematic, dynamic parameter adaption laws and disturbance observer are, respectively, designed as

$$u_i = -K_i s_i + Y_{di} \hat{\vartheta}_{di} - \hat{\mu}_i, \tag{14a}$$

$$\dot{\hat{\vartheta}}_{ki} = \Lambda_{ki} Y_{ki}^T \left(\frac{1}{\alpha_1} \dot{\tilde{x}}_i + 2\tilde{x}_i\right), \tag{14b}$$

$$\dot{\hat{\vartheta}}_{di} = -\Lambda_{di} Y_{di}^T s_i, \tag{14c}$$
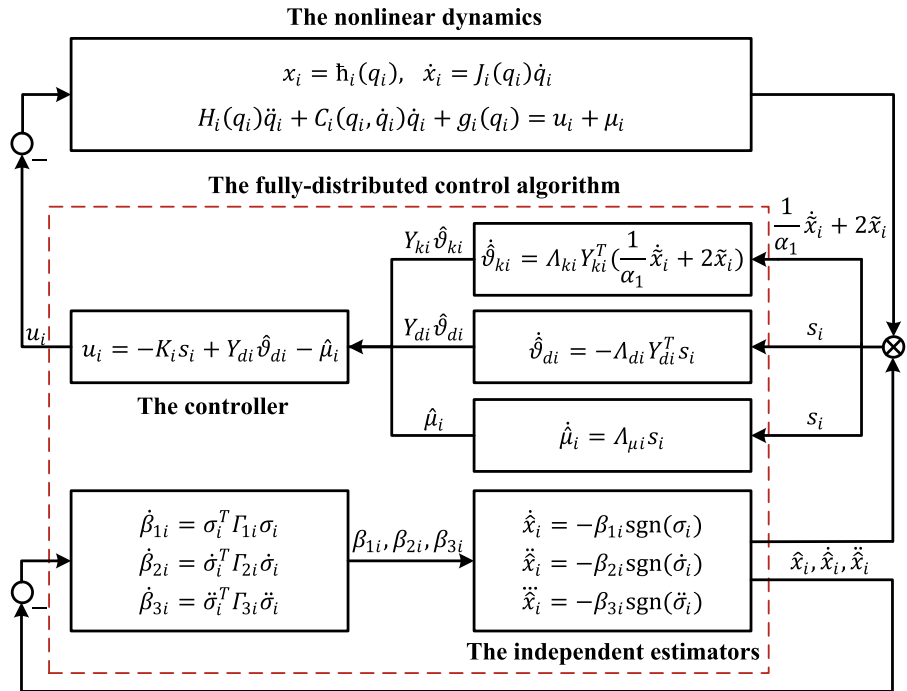
$$\dot{\hat{\mu}}_i = \Lambda_{\mu i} s_i, \tag{14d}$$

where $i \in \{1, \ldots, m\}$, $\hat{\mu}_i$ is the estimator of the disturbance μ_i, K_i, Λ_{ki}, Λ_{di}, $\Lambda_{\mu i}$ are symmetric positive definite matrices with proper dimensions and Y_{ki} and Y_{di} are abbreviations of $Y_{ki}(q_i, \dot{q}_{ri})$ and $Y_{di}(q_i, \dot{q}_i, \ddot{q}_{ri}, \dot{q}_{ri})$, respectively.

Remark 5 This paper considers the task-space formation tracking problem, while we must note that the reason for using auxiliary variables in joint space is that joint-space ones are more conveniently available since actuators and measurement sensors are always assembled at joints but the end effectors. Thus, this paper proposes a method to adopt the readily available auxiliary variables, *i.e.*, the so-called joint-space reference velocity $\dot{q}_{ri}$, acceleration $\ddot{q}_{ri}$ and sliding vector s_i in (12)–(13), to achieve the task-space positions x_i and velocities $\dot{x}_i$ that finally required in Definition 1 .

The interplay between the proposed fully distributed control algorithm and nonlinear dynamics is clearly shown in Fig. 1.

Remark 6 It can be easily concluded from Fig. 1 that the control systems are described as strongly nonlinear complex networks with parametric uncertainties and

The nonlinear dynamics

$$x_i = \hbar_i(q_i), \quad \dot{x}_i = J_i(q_i)\dot{q}_i$$
$$H_i(q_i)\ddot{q}_i + C_i(q_i, \dot{q}_i)\dot{q}_i + g_i(q_i) = u_i + \mu_i$$

The fully-distributed control algorithm

$$\frac{1}{\alpha_1}\dot{\tilde{x}}_i + 2\tilde{x}_i$$

$$Y_{ki}\hat{\vartheta}_{ki} \qquad \dot{\hat{\vartheta}}_{ki} = \Lambda_{ki}Y_{ki}^T(\frac{1}{\alpha_1}\dot{\tilde{x}}_i + 2\tilde{x}_i)$$

$$u_i \qquad u_i = -K_i s_i + Y_{di}\hat{\vartheta}_{di} - \hat{\mu}_i \qquad Y_{di}\hat{\vartheta}_{di} \qquad \dot{\hat{\vartheta}}_{di} = -\Lambda_{di}Y_{di}^T s_i \qquad s_i$$

The controller

$$\hat{\mu}_i \qquad \dot{\hat{\mu}}_i = \Lambda_{\mu i} s_i \qquad s_i$$

$$\dot{\beta}_{1i} = \sigma_i^T \Gamma_{1i}\sigma_i$$
$$\dot{\beta}_{2i} = \dot{\sigma}_i^T \Gamma_{2i}\dot{\sigma}_i \qquad \beta_{1i}, \beta_{2i}, \beta_{3i} \qquad \dot{\hat{x}}_i = -\beta_{1i}\mathrm{sgn}(\sigma_i)$$
$$\dot{\beta}_{3i} = \ddot{\sigma}_i^T \Gamma_{3i}\ddot{\sigma}_i \qquad \ddot{\hat{x}}_i = -\beta_{2i}\mathrm{sgn}(\dot{\sigma}_i) \qquad \hat{x}_i, \dot{\hat{x}}_i, \ddot{\hat{x}}_i$$
$$\dddot{\hat{x}}_i = -\beta_{3i}\mathrm{sgn}(\ddot{\sigma}_i)$$

The independent estimators

external disturbances. It thus motivates us to design a
concise nonlinear controller–estimator algorithm, con-
sisting of controller (14), independent distributed esti-
mators (9) and gain adaption laws (10), to solve the
task-space formation tracking problem of such nonlin-
ear Lagrangian dynamics. Although there is not any
feedback from systems (1) and controller (14) to esti-
mators (9), the control accuracy of estimators (9) can
also be well ensured by the designed gain adaption laws
(10). Meanwhile, the computing complexity and global
energy cost can be reduced to some extent. From the
physical and engineering point of view, gain adaption
law (10) implies that the supremums of ∞-norms $\dot{x}_0$,
$\ddot{x}_0$, $\dddot{x}_0$, can be unknown in prior, different from the case
that such information is assumed to be previously glob-
ally known to all agents in previous work [3,10,11].
Meanwhile, by utilizing disturbance observer (14d), the
supremum assumption of the external disturbances μ_i
in [10,11] is unnecessary, and the discontinuous effects
can be simultaneously handled. It thus concludes that
the nonlinear control problem in this paper can be
solved in a fully distributed manner.

Theorem 2 *For master robot $i \in \{1, \ldots, m\}$, suppose
Assumption 2 holds, with $J_i(q_i)$ and $\hat{J}_i(q_i)$ being non-
singular. Using (9), (10) and (14) for (1), the task-
space formation tracking of master robots with a single*

*leader defined in (7) can be asymptotically achieved,
i.e., $x_i - \delta_i - x_0 \to 0$, $\dot{x}_i - \dot{x}_0 \to 0$ as $t \to \infty$.*

Proof For master robot $i \in \{1, \ldots, m\}$, there exists
a finite time $t_1 > t_0$ to obtain the result presented in
Theorem 1; thus, the proof is proceeded as $t \in [t_0, t_1]$
and $t \in (t_1, \infty)$, respectively.

For $t \in [t_0, t_1]$, by a simple analysis, if the initial val-
ues $q_i(t_0)$, $\dot{q}_i(t_0) \in \mathcal{L}_\infty \cap \mathcal{L}_2$, one obtains q_i, $\dot{q}_i \in \mathcal{L}_\infty \cap$
$\mathcal{L}_2$ such that x_i, $\dot{x}_i \in \mathcal{L}_\infty \cap \mathcal{L}_2$ based on the nonsingu-
larity of $J_i(q_i)$. Similarly, if $\beta_{1i}(t_0)$, $\beta_{2i}(t_0)$, $\beta_{3i}(t_0) \in$
$\mathcal{L}_\infty \cap \mathcal{L}_2$ and $\hat{x}_i(t_0)$, $\dot{\hat{x}}_i(t_0)$, $\ddot{\hat{x}}_i(t_0) \in \mathcal{L}_\infty \cap \mathcal{L}_2$, one
obtains β_{1i}, β_{2i}, $\beta_{3i} \in \mathcal{L}_\infty \cap \mathcal{L}_2$ and $\hat{x}_i$, $\dot{\hat{x}}_i$, $\ddot{\hat{x}}_i \in$
$\mathcal{L}_\infty \cap \mathcal{L}_2$. Substituting the above values into (12) and
(13), one obtains that $\dot{q}_{ri}$, $\ddot{q}_{ri}$, $s_i \in \mathcal{L}_\infty \cap \mathcal{L}_2$ based
on the nonsingularity of $\hat{J}_i(q_i)$. Combining with Prop-
erties 1, 3 and 4, one obtains Y_{ki}, $Y_{di} \in \mathcal{L}_\infty \cap \mathcal{L}_2$.
Thus, by (14), $\hat{\vartheta}_{ki}$, $\hat{\vartheta}_{di}$, $\hat{\mu}_i \in \mathcal{L}_\infty \cap \mathcal{L}_2$ if the ini-
tial values $\hat{\vartheta}_{ki}(t_0)$, $\hat{\vartheta}_{di}(t_0)$, $\hat{\mu}_i(t_0) \in \mathcal{L}_\infty \cap \mathcal{L}_2$. There-
fore, it gives $u_i \in \mathcal{L}_\infty \cap \mathcal{L}_2$ such that $\ddot{q}_i \in \mathcal{L}_\infty \cap$
$\mathcal{L}_2$, i.e., $\ddot{x}_i \in \mathcal{L}_\infty \cap \mathcal{L}_2$. Finally, one achieves that
x_i, $\dot{x}_i$, $\ddot{x}_i$, s_i, $\hat{\vartheta}_{ki}$, $\hat{\vartheta}_{di}$, $\hat{\mu}_i \in \mathcal{L}_\infty \cap \mathcal{L}_2$ if $q_i(t_0)$, $\dot{q}_i(t_0)$,
$\beta_{1i}(t_0)$, $\beta_{2i}(t_0)$, $\beta_{3i}(t_0)$, $\hat{x}_i(t_0)$, $\dot{\hat{x}}_i(t_0)$, $\ddot{\hat{x}}_i(t_0)$, $\hat{\vartheta}_{ki}(t_0)$,
$\hat{\vartheta}_{di}(t_0)$, $\hat{\mu}_i(t_0) \in \mathcal{L}_\infty \cap \mathcal{L}_2$ as $t \in [t_0, t_1]$.

For $t \in (t_1, \infty)$, let $\tilde{\vartheta}_{di} \triangleq \vartheta_{di} - \hat{\vartheta}_{di}$, $\tilde{\mu}_i \triangleq \mu_i - \hat{\mu}_i$,
substituting (14a) into dynamics (1b) gives

$$H_i(q_i)\dot{s}_i = -C_i(q_i,\dot{q}_i)s_i - K_is_i - Y_{di}\tilde{\vartheta}_{di} + \tilde{\mu}_i, \quad (15)$$

Consider the following Lyapunov function candidate.

$$V_{1i}(t) = \frac{1}{2}s_i^T H_i(q_i)s_i + \frac{1}{2}\tilde{\vartheta}_{di}^T \Lambda_{di}^{-1}\tilde{\vartheta}_{di}$$
$$+ \frac{1}{2}\tilde{\mu}_i^T \Lambda_{\mu i}^{-1}\tilde{\mu}_i, \quad (16)$$

Taking the derivative of V_{1i} along (15) yields

$$\dot{V}_{1i}(t) = -s_i^T K_i s_i \leq 0,$$

which means $s_i \in \mathcal{L}_2 \cap \mathcal{L}_\infty$, $\tilde{\vartheta}_{di}, \tilde{\mu}_i \in \mathcal{L}_\infty$ as $t > t_1$. Note that one has obtained $s_i \in \mathcal{L}_2 \cap \mathcal{L}_\infty$, $\hat{\vartheta}_{di}, \hat{\mu}_i \in \mathcal{L}_\infty$ as $t \in [t_0, t_1]$ such that it gives $s_i \in \mathcal{L}_2 \cap \mathcal{L}_\infty$, $\hat{\vartheta}_{di}, \hat{\mu}_i \in \mathcal{L}_\infty$ for all $t \geq t_0$. Note that the details derivative of $V_{1i}(t)$ are given in "Appendix C1."

It is clear that $J_i s_i \in \mathcal{L}_2$ for $J_i, s_i \in \mathcal{L}_2$; thus, a positive constant K_1 exists and satisfies $K_1 \geq \int_{t_0}^t s_i^T(\varsigma) J_i^T(\varsigma) J_i(\varsigma)s_i(\varsigma)d\varsigma$. Then, consider the following Lyapunov function candidate.

$$V_{2i}(t) = \frac{1}{2}\tilde{x}_i^T \tilde{x}_i + \frac{1}{2}\tilde{\vartheta}_{ki}^T \Lambda_{ki}^{-1}\tilde{\vartheta}_{ki}$$
$$+ \frac{1}{\alpha_1}\left[K_1 - \int_{t_0}^t s_i^T(\varsigma) J_i^T(\varsigma) J_i(\varsigma)s_i(\varsigma)d\varsigma\right], \quad (17)$$

Differentiating (17) with respect to time yields

$$\dot{V}_{2i}(t) \leq -\frac{1}{2\alpha_1}\left(\dot{\tilde{x}}_i + \alpha_1\tilde{x}_i\right)^T \left(\dot{\tilde{x}}_i + \alpha_1\tilde{x}_i\right)$$
$$- \frac{\alpha_1}{2}\tilde{x}_i^T \tilde{x}_i - \frac{1}{2\alpha_1}(Y_{ki}\tilde{\vartheta}_{ki})^T Y_{ki}\tilde{\vartheta}_{ki} \leq 0,$$

which means $\tilde{\vartheta}_{ki} \in \mathcal{L}_\infty$, $\tilde{x}_i \in \mathcal{L}_2 \cap \mathcal{L}_\infty$, $\dot{\tilde{x}}_i \in \mathcal{L}_2 \cap \mathcal{L}_\infty$ (i.e., $\tilde{x}_i$ is uniformly continuous) as $t \geq t_0$. Note that the details derivative of $V_{2i}(t)$ are given in "Appendix C2."

By $\tilde{x}_i \in \mathcal{L}_2 \cap \mathcal{L}_\infty$ with $\tilde{x}_i$ being uniformly continuous, it is clear that $\tilde{x}_i \to 0$ as $t \to \infty$ based on Barbalat's lemma provided in Lemma 2. By (15), one obtains $\dot{s}_i \in \mathcal{L}_\infty$ such that $\ddot{q}_i \in \mathcal{L}_\infty$ based on the derivative of (13a), and thus $\ddot{\tilde{x}}_i \in \mathcal{L}_\infty$ (i.e., $\dot{\tilde{x}}_i$ is uniformly continuous). Combined with $\tilde{x}_i \in \mathcal{L}_\infty$ and Barbalat's lemma, it gives that $\dot{\tilde{x}}_i \to 0$ as $t \to \infty$. Note that $\tilde{x}_i = x_i - \delta_i - x_0$, $\dot{\tilde{x}}_i = \dot{x}_i - \dot{x}_0$ as $t \geq t_1$. Therefore, it follows Definition 1 that $\lim_{t\to\infty}(x_i - \delta_i - x_0) \to 0$ and $\lim_{t\to\infty}(\dot{x}_i - \dot{x}_0) \to 0$. It thus ends the proof. $\square$

Remark 7 In the first part, the asymptotic stability of position and velocity formation tracking errors is achieved by designing controller (14), which, in reality, is not necessary to guarantee the estimator $\hat{\vartheta}_{di}$ track the practical value ϑ_{di} accurately. Nevertheless, the convergence error between $\hat{\vartheta}_{di}$ and ϑ_{di} can also be reduced by sufficiently increasing the adaption gain Λ_{di} if necessary. Moreover, we must note that by increasing the adaption gain Λ_{di} to positive infinity, it may cause numerical instabilities and harmful effects for the system. Thus, in order to further reduce the estimator error and increase the system performance, persistence of excitation (PE) will be considered in our future work.

3.2 Task-space formation tacking with multiple leaders

For the second part, the task-space formation tracking of slave robots with multiple leaders is considered. and the superscript $*$ is employed to denote the slave robot $i \in \{m+1, \ldots, n\}$ for distinguishing from the above master robot $i \in \{1, \ldots, m\}$. Based on the above discussion, it gives the following similar estimators for the slave robots.

$$\dot{\hat{x}}_i^* = -\beta_{4i}\,\mathrm{sgn}\,(\varepsilon_i),$$
$$\ddot{\hat{x}}_i^* = -\beta_{5i}\,\mathrm{sgn}\,(\dot{\varepsilon}_i), \quad (18)$$
$$\dddot{\hat{x}}_i^* = -\beta_{6i}\,\mathrm{sgn}\,(\ddot{\varepsilon}_i),$$

where $i \in \{m+1, \ldots, n\}$, $\varepsilon_i = \sum_{j=1}^m \omega_{ij}(\hat{x}_i^* - \eta_i - \hat{x}_j) + \sum_{j=m+1}^n \omega_{ij}(\hat{x}_i^* - \hat{x}_j^* - \eta_i + \eta_j)$, the gains β_{4i}, β_{5i} and β_{6i} are generated from

$$\dot{\beta}_{4i} = \varepsilon_i^T \Gamma_{4i}\varepsilon_i,$$
$$\dot{\beta}_{5i} = \dot{\varepsilon}_i^T \Gamma_{5i}\dot{\varepsilon}_i, \quad (19)$$
$$\dot{\beta}_{6i} = \ddot{\varepsilon}_i^T \Gamma_{6i}\ddot{\varepsilon}_i,$$

By Theorem 1, one knows there exists a finite time, assumed as t_2, such that it follows $\varepsilon_i = 0$, $\dot{\varepsilon}_i = 0$, $\ddot{\varepsilon}_i = 0$, namely the vector form $(L_3 \otimes I_d)(\hat{X}_s^* - \eta + (L_3^{-1}L_2 \otimes I_d)\hat{X}_m) = 0$, $(L_3 \otimes I_d)(\dot{\hat{X}}_s^* + (L_3^{-1}L_2 \otimes I_d)\dot{\hat{X}}_m) = 0$, $(L_3 \otimes I_d)(\ddot{\hat{X}}_s^* + (L_3^{-1}L_2 \otimes I_d)\ddot{\hat{X}}_m) = 0$, where $\hat{X}_m = [\hat{x}_1; \ldots; \hat{x}_m]$, $\hat{X}_s^* = [\hat{x}_{m+1}^*; \ldots; \hat{x}_n^*]$, $\eta = [\eta_{m+1}; \ldots; \eta_n]$. Therefore, it follows that for $i \in \{m+1, \ldots, n\}$, there exist positive constants γ_j satisfying $\sum_{j=1}^m \gamma_j = 1$ such that $\hat{x}_i^*(t) - \eta_i - \sum_{j=1}^m \gamma_j\hat{x}_j(t) = 0$, $\dot{\hat{x}}_i^*(t) - \sum_{j=1}^m \gamma_j\dot{\hat{x}}_j(t) = 0$, $\ddot{\hat{x}}_i^*(t) - \sum_{j=1}^m \gamma_j\ddot{\hat{x}}_j(t) = 0$ in a finite time $t \in [t_0, t_2]$.

Afterward, the reference velocity, sliding vector and acceleration for slave robot $i \in \{m+1, \ldots, n\}$ are, respectively, described as

$$\dot{q}_{ri}^* \triangleq \hat{J}_i^{*+}\left(\dot{\hat{x}}_i^* - \alpha_2 \tilde{x}_i^*\right) + \left(I_{p_i}^* - \hat{J}_i^{*+}\hat{J}_i^*\right)\lambda_i^*, \quad (20a)$$

$$s_i^* \triangleq \dot{q}_i^* - \dot{q}_{ri}^* \triangleq \dot{q}_i^* - \hat{J}_i^{*+}\left(\dot{\hat{x}}_i^* - \alpha_2 \tilde{x}_i^*\right)$$
$$- \left(I_{p_i}^* - \hat{J}_i^{*+}\hat{J}_i^*\right)\lambda_i^*, \quad (20b)$$

$$\ddot{q}_{ri}^* \triangleq \dot{\hat{J}}_i^{*+}\left(\dot{\hat{x}}_i^* - \alpha_2 \tilde{x}_i^*\right) + \hat{J}_i^{*+}\left(\ddot{\hat{x}}_i^* - \alpha_2 \dot{\tilde{x}}_i^*\right)$$
$$+ \frac{d}{dt}\left(\left(I_{p_i}^* - \hat{J}_i^{*+}\hat{J}_i^*\right)\lambda_i^*\right), \quad (20c)$$

where α_2 is a positive constant, $\tilde{x}_i^* = x_i^* - \hat{x}_i^*$, $\dot{\tilde{x}}_i^* = \dot{x}_i^* - \dot{\hat{x}}_i^*$, $\lambda_i^* \in \mathbb{R}^{p_i}$ is an optimized convex function for the slave robots. Similarly, the control input, kinematic, dynamic parameter adaption laws and disturbance observer are, respectively, designed as

$$u_i^* = -K_i^* s_i^* + Y_{di}^* \hat{\vartheta}_{di}^* - \hat{\mu}_i^*, \quad (21a)$$

$$\dot{\hat{\vartheta}}_{ki}^* = \Lambda_{ki}^* Y_{ki}^{*T}\left(\frac{1}{\alpha_2}\dot{\tilde{x}}_i^* + 2\tilde{x}_i^*\right), \quad (21b)$$

$$\dot{\hat{\vartheta}}_{di}^* = -\Lambda_{di}^* Y_{di}^{*T} s_i^*, \quad (21c)$$

$$\dot{\hat{\mu}}_i^* = \Lambda_{\mu i}^* s_i^*, \quad (21d)$$

Theorem 3 *For slave robot $i \in \{m+1, \ldots, n\}$, suppose Assumption 2 holds, with $J_i^*(q_i)$ and $\hat{J}_i^*(q_i)$ being nonsingular. Using (18), (19) and (21) for (1), the task-space formation tracking of slave robots with multiple leaders defined in (8) can be asymptotically achieved, i.e., $x_i^* - \eta_i - \sum_{j=1}^m \gamma_j x_j \to 0$, $\dot{x}_i^* - \sum_{j=1}^m \gamma_j \dot{x}_j \to 0$ as $t \to \infty$.*

Proof For slave robot $i \in \{m+1, \ldots, n\}$, consider the following similar Lyapunov functions.

$$V_{3i}^*(t) = \frac{1}{2}s_i^{*T} H_i^*(q_i^*)s_i^* + \frac{1}{2}\tilde{\vartheta}_{di}^{*T}\Lambda_{di}^{*-1}\tilde{\vartheta}_{di}^*$$
$$+ \frac{1}{2}\tilde{\mu}_i^{*T}\Lambda_{\mu i}^{*-1}\tilde{\mu}_i^*, \quad (22a)$$

$$V_{4i}^*(t) = \frac{1}{2}\tilde{x}_i^{*T}\tilde{x}_i^* + \frac{1}{2}\tilde{\vartheta}_{ki}^{*T}\Lambda_{ki}^{*-1}\tilde{\vartheta}_{ki}^*$$
$$+ \frac{1}{\alpha_2}\left[K_2 - \int_{t_0}^t s_i^{*T}(\varsigma)J_i^{*T}(\varsigma)J_i^*(\varsigma)s_i^*(\varsigma)d\varsigma\right], \quad (22b)$$

By a similar analysis performed in Theorem 2, one obtains $s_i^*, \dot{s}_i^* \in \mathcal{L}_\infty$ and $\tilde{\vartheta}_{ki}^*, \tilde{\vartheta}_{di}^*, \tilde{\mu}_i^* \in \mathcal{L}_\infty$ as $t \geq t_0$, such that one finally obtains $s_i^*, \tilde{\vartheta}_{ki}^* \to 0$ as $t \to \infty$. Then, rewrite (20b) as the following vector form.

$$\dot{\tilde{X}}_s^* = -\alpha_2 \tilde{X}_s^* + J^* S^* + Y_k^* \tilde{\vartheta}_k^*, \quad (23)$$

where $\tilde{X}_s^* = X_s^* - \eta + \left(L_3^{-1}L_2 \otimes I_d\right)\hat{X}_m$, $J^*, Y_k^* \in \mathbb{R}^{(n-m)d \times (n-m)p_i}$ are block matrices of J_i^*, Y_{ki}^*, respectively. $S^*, \tilde{\vartheta}_k^* \in \mathbb{R}^{(n-m)p_i}$ are the column stack vectors of $s_i^*, \tilde{\vartheta}_{ki}^*$, respectively. Based on $S^*, \tilde{\vartheta}_k^* = 0_{(n-m)p_i}$ and input-to-state stability theory provided in Lemma 3, one says (23) is input-to-state stable at the origin $\tilde{X}_s^* = \dot{\tilde{X}}_s^* = 0_{(n-m)d}$. Thus, one obtains $\tilde{X}_s^*, \dot{\tilde{X}}_s^* \to 0$, i.e., $x_i^*(t) - \eta_i - \sum_{j=1}^m \gamma_j \hat{x}_j(t) \to 0$, $\dot{x}_i^*(t) - \sum_{j=1}^m \gamma_j \dot{\hat{x}}_j(t) \to 0$ as $t \to \infty$. Combining with $\hat{x}_j(t) - \delta_j - x_0(t) = 0$, $\dot{\hat{x}}_j(t) - \dot{x}_0(t) = 0$ for master robot $j \in \{1, \ldots, m\}$ as $t \geq t_1$ shown in Theorem 2, then, it follows that presented in Definition 2. This completes the proof. □

Remark 8 Likewise, it is not necessary to obtain the accurate value of the finite time t_2 in the proof of Theorem 3. Moreover, the formation tracking of slave robots with multiple leaders can also be obtained with a redefined value ε_i right after 18.

$$\varepsilon_i = \sum_{j=1}^m \omega_{ij}(\hat{x}_i^* - \eta_i - x_j)$$
$$+ \sum_{j=m+1}^n \omega_{ij}(\hat{x}_i^* - \hat{x}_j^* - \eta_i + \eta_j),$$

where the actual positions x_j of master robots are introduced to replace the estimated ones.

By Theorems 2 and 3, Table 1 shows the control process of the fully distributed control algorithm. Note that the following subprocesses (1) and (2) in each step are carried out simultaneously.

It is worth pointing out that the formation tracking of NHRS can also be achieved by a control algorithm with another kinematic parameter adaption law.

Corollary 1 *For robot $i \in \{1, \ldots, n\}$, suppose Assumption 2 holds, with $J_i(q_i)$ and $\hat{J}_i(q_i)$ being nonsingular. Respectively replace $\dot{\hat{\vartheta}}_{ki}$ in (14b) and $\dot{\hat{\vartheta}}_{ki}^*$ in (21b) with*

$$\dot{\hat{\vartheta}}_{ki} = \Lambda_{ki} Y_{ki}^T(q_i, \dot{q}_i)\left(\frac{1}{\alpha_1}\dot{\tilde{x}}_i + 2\tilde{x}_i\right),$$

$$\dot{\hat{\vartheta}}_{ki}^* = \Lambda_{ki}^* Y_{ki}^{*T}(q_i^*, \dot{q}_i^*)\left(\frac{1}{\alpha_1}\dot{\tilde{x}}_i^* + 2\tilde{x}_i^*\right),$$

where $\dot{q}_i$ and $\dot{q}_i^*$ are used to replace $\dot{q}_{ri}$ in Y_{ki}^T and $\dot{q}_{ri}^*$ in Y_{ki}^{*T}, respectively. Combined with corresponding control inputs, dynamic parameter adaption law and disturbance observer, the task-space formation tracking of NHRS defined in (7) and (8) can be asymptotically achieved.

Table 1 The control process of the fully distributed task-space formation tracking control algorithm

Algorithm:	Fully distributed task-space formation tracking control algorithm
Main input :	$x_r, \alpha, \beta_i, \Gamma_i, \Lambda_{ki}, \Lambda_{di}, \Lambda_{\mu i}, K_i, \mu_i, \delta_i, \eta_i$
Main output :	$x_i, \dot{x}_i$

Step 1.	Initialization of system parameters:
	(1) for master robots $i \in \{1, \ldots, m\}$, suppose $q_i(t_0), \dot{q}_i(t_0), \beta_{1i}(t_0), \beta_{2i}(t_0), \beta_{3i}(t_0), \hat{x}_i(t_0), \dot{\hat{x}}_i(t_0), \ddot{\hat{x}}_i(t_0), \hat{\vartheta}_{ki}(t_0),$ $\hat{\vartheta}_{di}(t_0), \hat{\mu}_i(t_0) \in \mathcal{L}_\infty \cap \mathcal{L}_2;$
	(2) for slave robots $i \in \{m + 1, \ldots, n\}$, suppose $q_i^*(t_0), \dot{q}_i^*(t_0), \beta_{4i}(t_0), \beta_{5i}(t_0), \beta_{6i}(t_0), \hat{x}_i^*(t_0), \dot{\hat{x}}_i^*(t_0), \ddot{\hat{x}}_i^*(t_0),$ $\hat{\vartheta}_{ki}^*(t_0), \hat{\vartheta}_{di}^*(t_0), \hat{\mu}_i^*(t_0) \in \mathcal{L}_\infty \cap \mathcal{L}_2;$
Step 2.	Definition of sliding-mode estimators and gain adaption laws:
	(1) for master robots, define $\hat{x}_i, \dot{\hat{x}}_i, \ddot{\hat{x}}_i$ and $\beta_{1i}, \beta_{2i}, \beta_{3i}, \delta_i$, such that $\hat{x}_i = \delta_i + x_0, \dot{\hat{x}}_i = \dot{x}_0, \ddot{\hat{x}}_i = \ddot{x}_0$ as $t \geq t_1;$
	(2) for slave robots, define $\hat{x}_i^*, \dot{\hat{x}}_i^*, \ddot{\hat{x}}_i^*$ and $\beta_{4i}, \beta_{5i}, \beta_{6i}, \varepsilon_i, \gamma_j$, such that $\hat{x}_i^* = \eta_i + \sum_{j=1}^m \gamma_j \hat{x}_j, \dot{\hat{x}}_i^* = \sum_{j=1}^m \gamma_j \dot{\hat{x}}_j,$ $\ddot{\hat{x}}_i^* = \sum_{j=1}^m \gamma_j \ddot{\hat{x}}_j$ as $t \geq t_2;$
Step 3.	Design of control inputs and adaption laws:
	(1) for master robots, design $\alpha_1, \lambda_i, K_i, \Lambda_{ki} \Lambda_{di}$ and $\Lambda_{\mu i}$, thus $\tau_i, \dot{\hat{\vartheta}}_{ki}, \dot{\hat{\vartheta}}_{di}$ and $\dot{\hat{\mu}}_i$ are obtained;
	(2) for slave robots, design $\alpha_2, \lambda_i^*, K_i^*, \Lambda_{ki}^*, \Lambda_{di}^*$ and $\Lambda_{\mu i}^*$, thus $\tau_i^*, \dot{\hat{\vartheta}}_{ki}^*, \dot{\hat{\vartheta}}_{di}^*$ and $\dot{\hat{\mu}}_i^*$ are obtained;
Step 4.	Conclusions of the control process:
	(1) for master robots, by $V_{1i}(t), V_{2i}(t)$ and Barbalat's lemma, the control objective proposed in Definition 1 is achieved;
	(2) for slave robots, by $V_{3i}^*(t), V_{4i}^*(t)$ and input-to-state stability Theory, the control objective proposed in Definition 2 is achieved.

Meanwhile, not only the fixed-topology problems but also the cases with dynamical topologies can be solved via the above algorithms involving dynamically changed communication topologies.

Corollary 2 *Suppose Assumption* 2 *holds. Replace the constant* ω_{ij} *and* b_i *in Theorems* 2 *and* 3 *with the time-varying weights* $\omega_{ij}(t)$ *and* $b_i(t)$, *such that the formation tracking of master and slave robots with dynamical topology can be achieved.*

Furthermore, the algorithm can also be applied to address the formation-containment problems by some simple transformation.

Corollary 3 *Suppose that Assumption* 2 *and Theorem* 2 *hold. Replace* ε_i *in Theorem* 3 *with* $\varepsilon_i = \sum_{j=1}^n \omega_{ij}(\hat{x}_i^* - \hat{x}_j)$, *and use* (18), (19) *and* (21) *for* (1), *the task-space containment of slave robots can be asymptotically achieved, i.e.,* $x_i^* - \sum_{j=1}^m \gamma_j x_j \to 0,$ $\dot{x}_i^* - \sum_{j=1}^m \gamma_j \dot{x}_j \to 0$ *as* $t \to \infty$, *such that the formation-containment control of NHRS is achieved.*

Last but not least, consensus problems can also be solved as declared in Corollary 4.

Corollary 4 *Suppose Assumption* 2 *holds. Replace* σ_i *in Theorem* 2 *with* $\sigma_i = \sum_{j=1}^m \omega_{ij}(\hat{x}_i - \hat{x}_j) + b_i(\hat{x}_i - x_0)$, *as well as* ε_i *in Theorem* 3 *with* $\varepsilon_i = \sum_{j=1}^m \omega_{ij}(\hat{x}_i^* - \hat{x}_j) + \sum_{j=m+1}^n \omega_{ij}(\hat{x}_i^* - \hat{x}_j^*)$, *thus, the consensus of NHRS is achieved by using corresponding control algorithms for* (1), *i.e.,* $x_i - x_0 \to 0,$ $\dot{x}_i - \dot{x}_0 \to 0, i \in \{1, \ldots, m\}$, *and* $x_i^* - \sum_{j=1}^m \gamma_j x_j \to 0, \ddot{x}_i^* - \sum_{j=1}^m \gamma_j \dot{x}_j \to 0, i \in \{m+1, \ldots, n\}$ *as* $t \to \infty$.

Proof The proofs of above corollaries are similar to the analysis in Theorems 2 and 3 and are omitted here for saving space. □

Remark 9 In this paper, system (1) is the global control objective, which is employed to achieve the control problems given in Definitions 1 and 2, while system (11) is the local control objective, which is adopted for obtaining the estimators defined in (9) and (18). Note that the estimators are first obtained, then by invoking them for the controllers (14) and (21), respectively, the formation tracking of system (1) can be finally achieved.

Remark 10 The reasons for choosing multiple master robots rather than one are listed as follows. For practi-

cal applications, it is more adaptable and reliable for the system with multiple master robots for the events with any single-master robot is disabled for some known or unknown issues. For theory research, it is not only a more robust and flexible system but also a challenging problem since the existence of distributed control manner among the robots. Moreover, it is more convenient for the results to be extended to multi-task problems.

Remark 11 The challenges and necessary for investigating the formation tracking problem with both single and multiple leaders are summarized as follows. First, the design of estimators (9) and gain adaption laws (10) in the single-leader case (Sect. 3.1) only requires the known parameters $x_0, \dot{x}_0, \ddot{x}_0$, while (18) and (19) in multiple-leader case (Sect. 3.2) are based on the unknown results $x_j, \dot{x}_j, \ddot{x}_j, j \in \{1, \ldots, m\}$ obtained in Sect. 3.1, such that the problem with both single and multiple leaders is more challenging. Overall, it is more convenient for the combined results to be extended to address multi-task problems, such that it is useful and necessary to investigate the problem with both single and multiple leaders.

Remark 12 Compared to the formation tracking problems [15–18] and fully distributed problems [16,17, 22–25] of linear or homogeneous systems with a single leader, this paper develops fully distributed control algorithms for NHRSs to, respectively, achieve task-space formation with single and multiple time-varying leaders, which enriches the scenarios of coordination behaviors. In contrast to the formation tracking problem of linear or homogeneous systems with multiple

leaders [19–21], this paper focuses on Lagrangian systems with the nonlinear heterogeneous properties, parametric uncertainties and external disturbances. Superior to the control algorithms developed in [10,11], this paper develops fully distributed control algorithms with gain and disturbance-avoid adaption laws, which do not require the upper bound assumption of reference states and external disturbances. Unlike the fully distributed control algorithms, relying on the assumptions that the communication topologies are undirected or strongly connected [24–27], this paper develops fully distributed control algorithms under a milder assumption. Moreover, note that by employing time delays in the communication channels, the proposed control algorithms can be further extended to teleoperation robotic systems considered in [12,13].

4 Numerical examples

In this section, example 1 is performed to demonstrate the validity of the main results obtained in the above sections, while example 2 is given to show the comparisons with previous results in [10].

Example 1 Without loss of generality, assume there exist six planar master robots and eight planar slave robots, displayed in Fig. 2, in NHRS, and the numbers of nonredundant and redundant robots in each group are, respectively, identical. The physical parameters of robot $i \in \{1, \cdots, 14\}$ are given in Table 2, where m_i, l_i, r_i and I_i, respectively, denote
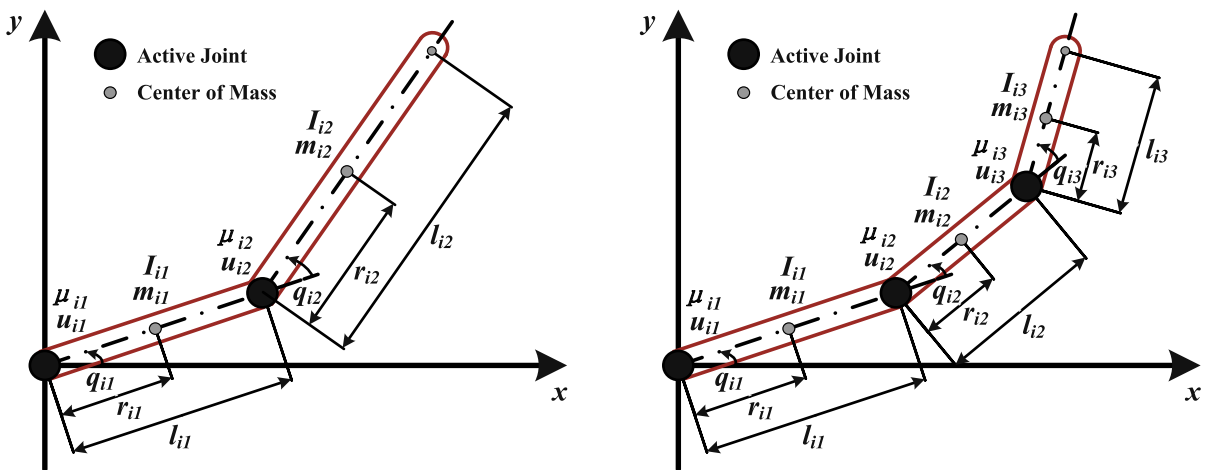

Fig. 2 The planar nonredundant and redundant robots in NHRS

Table 2 The physical parameters of NHRS

i-th Robot	m_i (kg)	l_i (m)	r_i (m)	I_i (kg m^2)
$i = 1, 2, 3, 7, 8, 9, 10$	1.4, 1.6	1.4, 1.6	0.7, 0.8	0.27, 0.41
$i = 4, 5, 6, 11, 12, 13, 14$	1.4, 1.0, 0.8	1.4, 1.0, 0.8	0.7, 0.5, 0.4	0.27, 0.1, 0.05

Table 3 The constant dynamic parameters of NHRS

i-th Robot	ϑ_{di}
$i = 1, 2, 3, 7, 8, 9, 10$	$\vartheta_{di1} = m_{i1}r_{i1}^2 + m_{i2}\left(l_{i1}^2 + r_{i2}^2\right) + I_{i1} + I_{i2}, \vartheta_{di2} = m_{i2}l_{i1}r_{i2},$ $\vartheta_{di3} = m_{i2}r_{i2}^2 + I_{i2}, \vartheta_{di4} = m_{i1}r_{i1} + m_{i2}l_{i1}, \vartheta_{di5} = m_{i2}r_{i2}$
$i = 4, 5, 6, 11, 12, 13, 14$	$\vartheta_{di1} = m_{i1}r_{i1}^2 + (m_{i2} + m_{i3})l_{i1}^2 + I_{i1}, \vartheta_{di2} = m_{i2}r_{i2}^2 + m_{i3}l_{i2}^2 + I_{i2},$ $\vartheta_{di3} = m_{i2}r_{i2}l_{i1} + m_{i3}l_{i2}l_{i1}, \vartheta_{di4} = m_{i3}r_{i3}^2 + I_{i3}, \vartheta_{di5} = m_{i3}r_{i3}l_{i1},$ $\vartheta_{di6} = m_{i3}r_{i3}l_{i2}, \vartheta_{di7} = m_{i1}r_{i1} + m_{i2}l_{i1} + m_{i3}l_{i1},$ $\vartheta_{di8} = m_{i2}r_{i2} + m_{i3}l_{i2}, \vartheta_{di9} = m_{i3}r_{i3}$

Table 4 The inertia matrix of NHRS

i-th Robot	$H_i(q_i)$
$i = 1, 2, 3, 7, 8, 9, 10$	$H_{11} = \vartheta_{di1} + 2\vartheta_{di2}\cos q_{i2}, H_{12} = H_{21} = \vartheta_{di3} + \vartheta_{di2}\cos q_{i2}, M_{22} = \vartheta_{di3}$
$i = 4, 5, 6, 11, 12, 13, 14$	$H_{11} = \vartheta_{di1} + \vartheta_{di2} + \vartheta_{di4} + 2\vartheta_{di3}\cos q_2 + 2\vartheta_{di5}\cos(q_2 + q_3) + 2\vartheta_{di6}\cos q_3,$ $H_{12} = H_{21} = \vartheta_{di2} + \vartheta_{di4} + \vartheta_{di3}\cos q_2 + \vartheta_{di5}\cos(q_2 + q_3) + 2\vartheta_{di6}\cos q_3,$ $H_{13} = H_{31} = \vartheta_{di4} + \vartheta_{di5}(q_2 + q_3) + \vartheta_{di6}\cos q_3, H_{33} = \vartheta_{di4}, H_{22} = \vartheta_{di2} + \vartheta_{di4} + 2\vartheta_{di6}\cos q_3,$ $H_{23} = H_{32} = \vartheta_{di4} + \vartheta_{di6}\cos q_3$

Table 5 The Coriolis–centrifugal matrix of NHRS

i-th Robot	$C_i(q_i, \dot{q}_i)$
$i = 1, 2, 3, 7, 8, 9, 10$	$C_{11} = -\vartheta_{di2}\dot{q}_{i2}\sin q_{i2}, C_{12} = -\vartheta_{di2}(\dot{q}_{i1} + \dot{q}_{i2})\sin q_{i2},$ $C_{21} = \vartheta_{di2}\dot{q}_{i1}\sin q_{i2}, C_{22} = 0$
$i = 4, 5, 6, 11, 12, 13, 14$	$C_{11} = -\vartheta_{di3}\dot{q}_2\sin q_2 - \vartheta_{di5}(\dot{q}_2 + \dot{q}_3)\sin(q_2 + q_3) - \vartheta_{di6}\dot{q}_3\sin q_3,$ $C_{12} = -\vartheta_{di3}(\dot{q}_1 + \dot{q}_2)\sin q_2 - \vartheta_{di5}(\dot{q}_1 + \dot{q}_2 + \dot{q}_3)\sin(q_2 + q_3) - \vartheta_{di6}\dot{q}_3\sin q_3,$ $C_{13} = -(\vartheta_{di5}\sin(q_2 + q_3) + \vartheta_{di6}\sin q_3)(\dot{q}_1 + \dot{q}_2 + \dot{q}_3),$ $C_{21} = \vartheta_{di3}\dot{q}_1\sin q_2 + \vartheta_{di5}\dot{q}_1\sin(q_2 + q_3) - \vartheta_{di6}\dot{q}_3\sin q_3,$ $C_{22} = -\vartheta_{di6}\dot{q}_3\sin q_3, C_{23} = -\vartheta_{di6}(\dot{q}_1 + \dot{q}_2 + \dot{q}_3)\sin q_3,$ $C_{31} = \vartheta_{di5}\dot{q}_1\sin(q_2 + q_3) + \vartheta_{di6}(\dot{q}_1 + \dot{q}_2)\sin q_3,$ $C_{32} = \vartheta_{di6}(\dot{q}_1 + \dot{q}_2)\sin q_3, C_{33} = 0$

the mass, length, distance between the joint and the center of mass, and the moment of inertia around its center of mass [10]. The constant dynamic parameters of NHRS are displayed in Table 3 such that by Property 4, the dynamics (1b) can be linearized with respect to ϑ_{di}, with the dynamic parameters obtained and displayed in Tables 4, 5 and 6, where for $i \in \{1, 2, 3, 7, 8, 9, 10\}$, $H_i(q) = [H_{11}, H_{12}; H_{21}, H_{22}]$, $C_i(q, \dot{q}) = [C_{11}, C_{12}; C_{21}, C_{22}]$, $g_i(q) = [g_1; g_2]$; and for $i \in \{4, 5, 6, 11, 12, 13, 14\}$, $H_i(q) = [H_{11},$ $H_{12}, H_{13}; H_{21}, H_{22}, H_{23}; H_{31}, H_{32}, H_{33}], C_i(q, \dot{q}) =$ $[C_{11}, C_{12}, C_{13}; C_{21}, C_{22}, C_{23}; C_{31}, C_{32}, C_{33}], g_i(q)$ $= [g_1; g_2; g_3]$. Note that the gravitational acceleration g in gravitational torque $g_i(q_i)$ satisfies $g = 9.8kg \cdot m^2$.

As shown in Fig. 3, a directed topology $\mathcal{G}$ containing a directed spanning tree is used to describe the communications of NHRS, where node 0, nodes 1–6 and nodes 7–14, respectively, denote the virtual leader, the master robots and the slave robots, with the three types of desired configurations shown in Fig. 4. Note that $\delta_1 =$

Table 6 The gravitational torque of NHRS

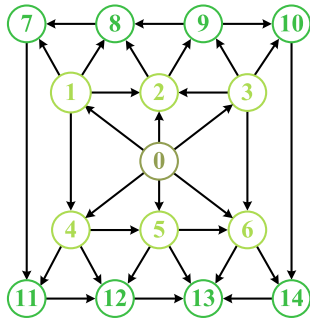| i-th Robot	$g_i(q_i)$
$i = 1, 2, 3, 7, 8, 9, 10$	$g_1 = \vartheta_{di4}g\cos q_{i1} + \vartheta_{di5}g\cos(q_{i1}+q_{i2})$, $g_2 = \vartheta_{di5}g\cos(q_{i1}+q_{i2})$
$i = 4, 5, 6, 11, 12, 13, 14$	$g_1 = \vartheta_{di7}g\cos q_{i1} + \vartheta_{di8}g\cos(q_{i1}+q_{i2}) + \vartheta_{di9}g\cos(q_{i1}+q_{i2}+q_{i3})$,
	$g_2 = \vartheta_{di8}g\cos(q_{i1}+q_{i2}) + \vartheta_{di9}g\cos(q_{i1}+q_{i2}+q_{i3})$,
	$g_3 = \vartheta_{di9}g\cos(q_{i1}+q_{i2}+q_{i3})$

Fig. 3 The directed communication topology $\mathcal{G}$ of the nonlinear system

$[0.05; 0.09]$, $\delta_2 = [0.1; 0]$, $\delta_3 = [0.05; -0.09]$, $\delta_4 = -\delta_1$, $\delta_5 = -\delta_2$, $\delta_6 = -\delta_3$. $\eta_1 = [0.09; 0.21]$, $\eta_2 = [0.25; 0.1]$, $\eta_3 = [0.25; -0.1]$, $\eta_4 = [0.09; -0.21]$, $\eta_5 = -\eta_1$, $\eta_6 = -\eta_2$, $\eta_7 = -\eta_3$, $\eta_8 = -\eta_4$. Moreover, for $t \geq t_0 = 0$, the task-space position of virtual leader is given as follows.

$$x_0(t) = [1.0 + 1.0\sin(0.2t); \ -1.0 - 1.0\cos(0.2t)].$$

For the robots in NHRS, set $t_0 = 0$ and initialize the joint-space positions $q_i(0)$ as $[5; -1]$, $[5; 6]$, $[5; 12]$, $[5; -1; 13]$, $[5; 5; 1]$, $[5; 6; 6]$, $[11; 6]$, $[4; 8]$, $[4; 14]$, $[5; 24]$, $[4; 1; 13]$, $[4; 1; 19]$, $[4; 7; 1]$, $[4; 2; 5]$. Initialize velocities $\dot{q}_i(0)$ of nonredundant

and redundant robots as $[1; 2]$ and $[1; 2; 3]$, respectively. Initialize estimated kinematic parameters $\hat{\vartheta}_{ki}(0)$ of nonredundant and redundant robots as $[0.4; 0.3]$ and $[0.4; 0.3; .2]$, respectively. Initialize estimated dynamic parameters $\hat{\vartheta}_{di}(0)$, estimated disturbances $\hat{\mu}_i(0)$, gains $\beta_i(0)$ and sliding-mode estimators $\hat{x}_i(0)$, $\hat{\dot{x}}_i(0)$, $\hat{\ddot{x}}_i(0)$ as zero. Design $\alpha_1 = \alpha_2 = 0.2$, $\Gamma_i = 800I_2$. The elements of disturbances μ_i are randomly selected from $[-1, 1]$. Meanwhile, for robot $i \in \{1, 2, 3, 7, 8, 9, 10\}$, design $K_i = 8I_2$, $\Lambda_{ki} = 55I_2$, $\Lambda_{di} = 55I_5$ and $\Lambda_{\mu i} = 55I_2$; for robot $i \in \{4, 5, 6, 11, 12, 13, 14\}$, design $\lambda_i = [0; 0.9(\pi/3 - q_{i2}); 0]$, $K_i = 8I_3$, $\Lambda_{ki} = 55I_3$, $\Lambda_{di} = 55I_9$ and $\Lambda_{\mu i} = 55I_3$.

The example results of the formation tracking problem are shown in Figs. 5, 6, 7, 8, 9, 10, 11, 12 and 13. Figures 5, 8, 11 and 6, 9, 12, respectively, depict task-space position and velocity tracking errors $\tilde{x}_i$ and $\tilde{\dot{x}}_i$, and Figs. 7, 10, 13 depict the task-space formation tracking performance of the three cases shown in Fig. 4. By Figs. 5, 8, 11 and Figs. 6, 9, 12, one sees that all the task-space positions and velocities, respectively, reach the agreement within $t = 15$ seconds. In Figs. 7, 10 and 13, the heavy line and pentagram are used for describing the reference trajectory, the solid line, rhombus and asterisk for the master robots, and the dashed
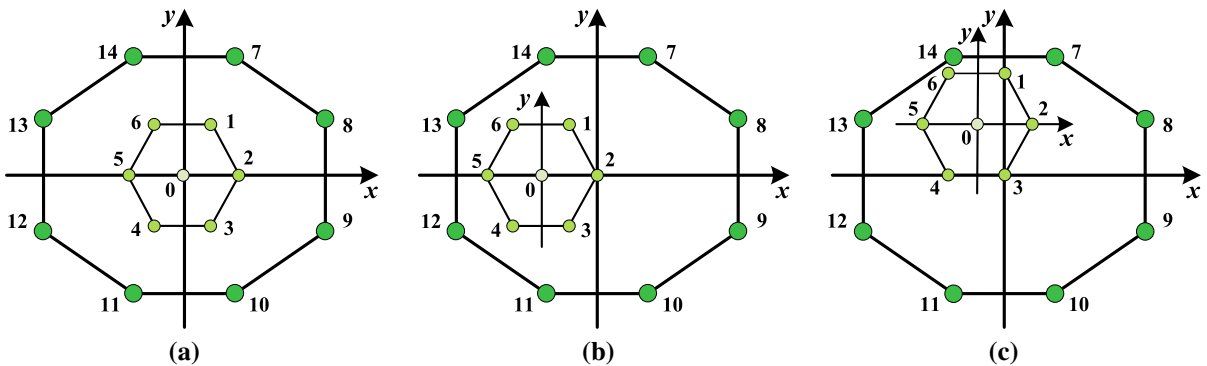

Fig. 4 The desired configurations of the robots in NHRS. **a** The case with every $\gamma_j = \frac{1}{6}$. **b** The case with $\gamma_2 = 1$. **c** The case with $\gamma_3 = 1$

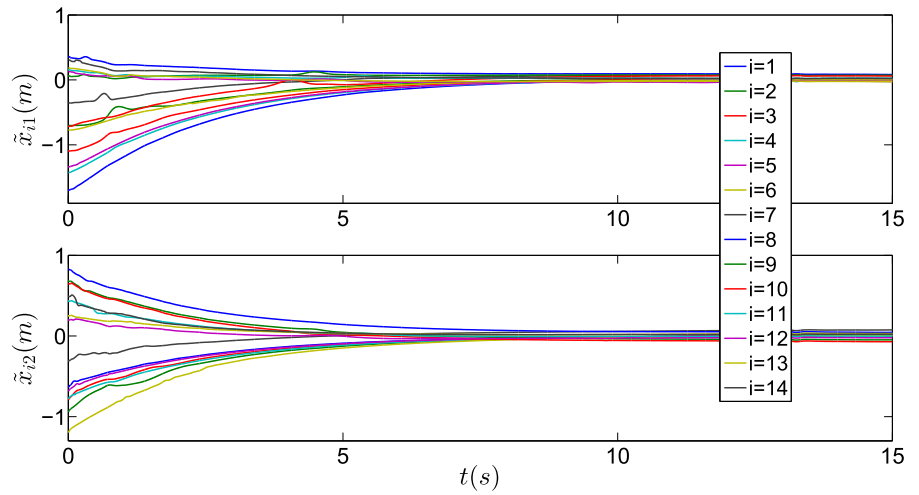**Fig. 5** The task-space position tracking errors $\tilde{x}_i$ of the robots in case (**a**)

Fig. 6 The task-space velocity tracking errors $\dot{\tilde{x}}_i$ of the robots in case (**a**)
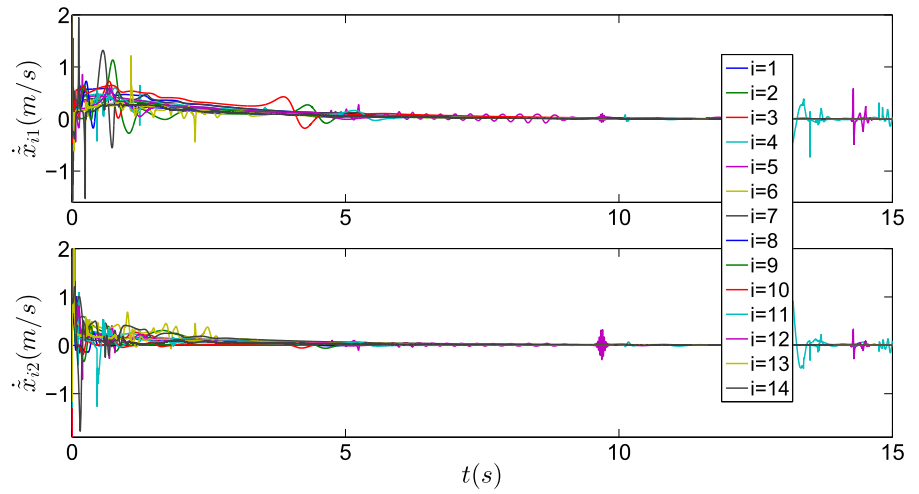

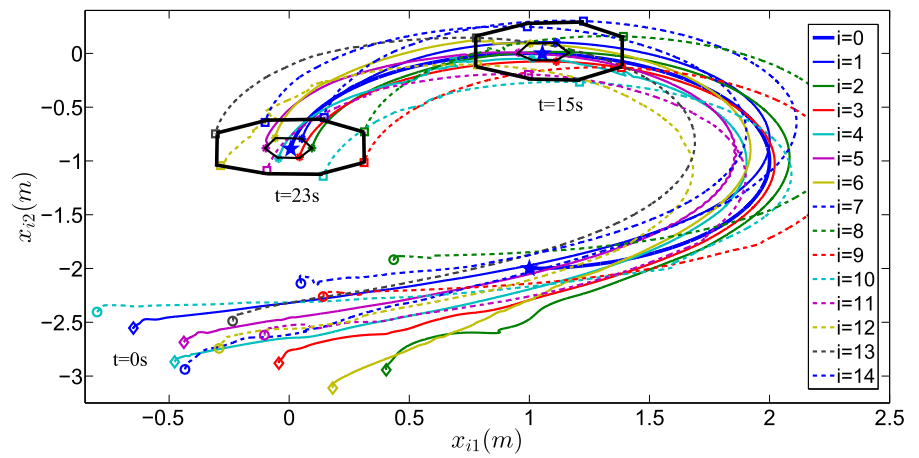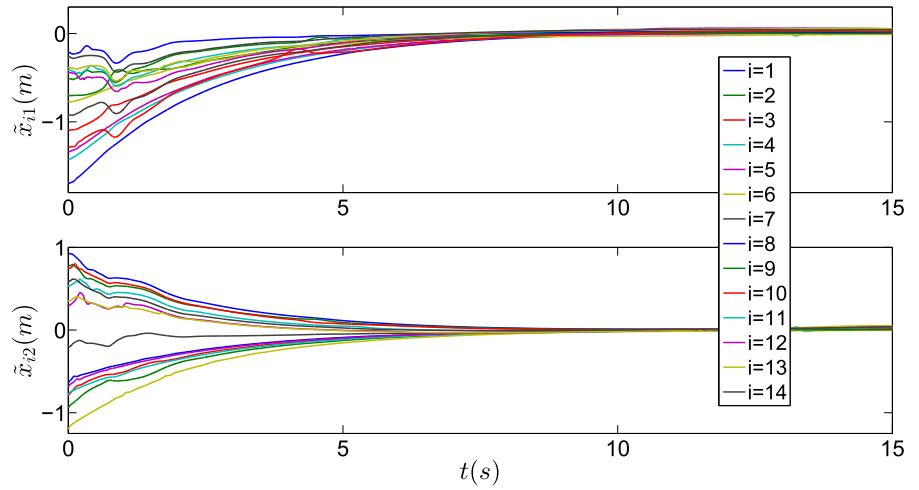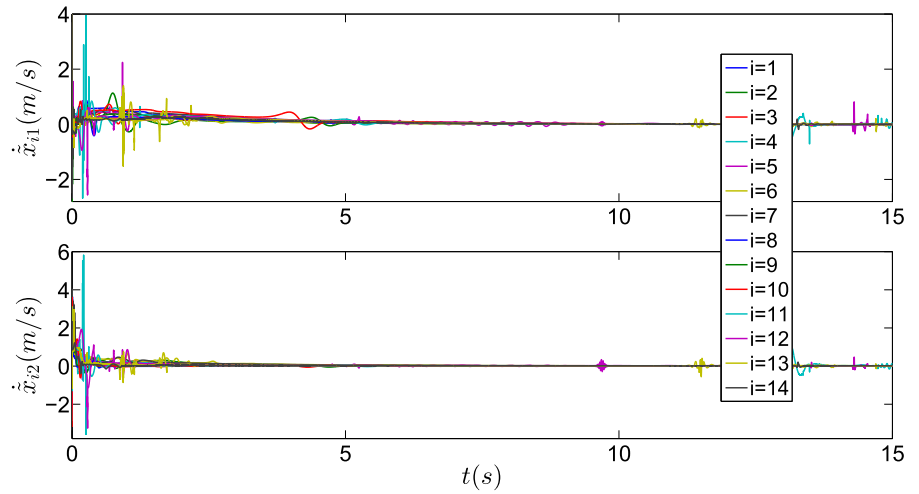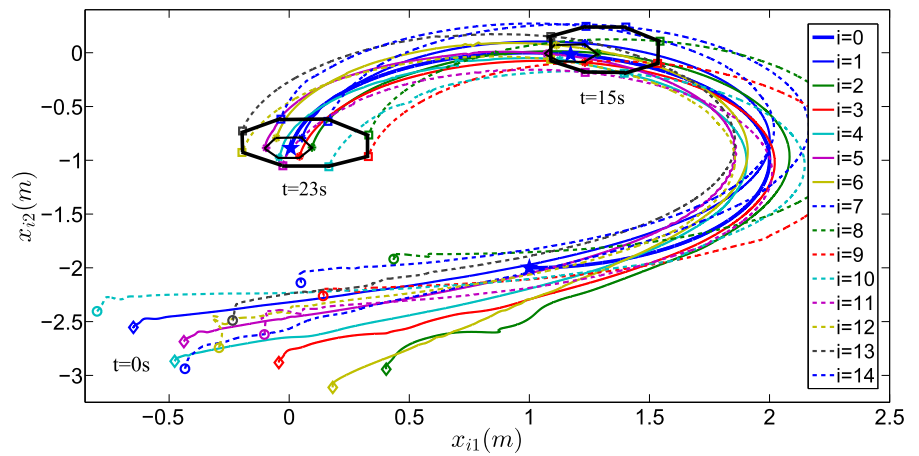**Fig. 7** The task-space formation tracking performance of case (**a**)

Fig. 8 The task-space position tracking errors $\tilde{x}_i$ of the robots in case (**b**)
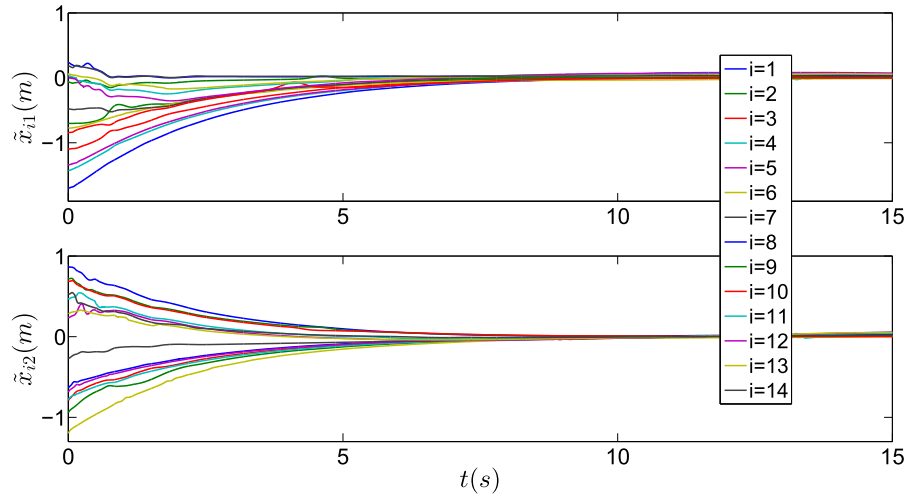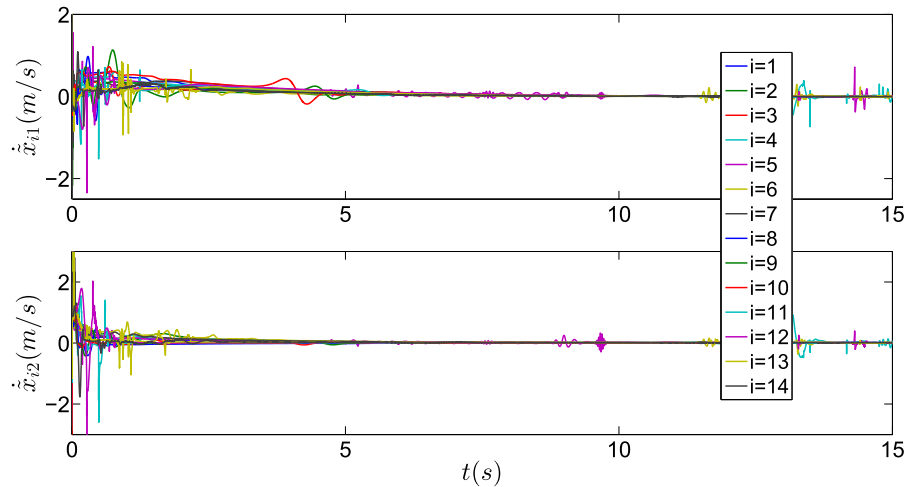

Fig. 9 The task-space velocity tracking errors $\dot{\tilde{x}}_i$ of the robots in case (**b**)

Fig. 10 The task-space formation tracking performance of case (**b**)

Fig. 11 The task-space position tracking errors $\tilde{x}_i$ of the robots in case (**c**)

Fig. 12 The task-space velocity tracking errors $\dot{\tilde{x}}_i$ of the robots in case (**c**)

line, circle and quadrate for the slave robots. At the initial time, the positions of all the robots are decentralized. Then, one sees that the three cases shown in Fig. 4 are, respectively, achieved within $t = 23$ seconds, which is an interesting advantage from a practical point of view since the algorithms proposed in this paper can be applied in the cases, where dangerous tasks, including reconnaissance and attack, can be accomplished by the unmanned slave robots outside, while the manned master robots can be protected by the constructed defensive systems.

Example 2 To show the advantages of the obtained results, the consensus control algorithm designed in [10] is extended to formation tracking cases to make a comparison. The control algorithm is designed as

$$u_i = Y_{di}\hat{\vartheta}_{di} - K_{si}s_i - K_{\mu i}\,\mathrm{sgn}\,(s_i),$$

$$\dot{\hat{\vartheta}}_{ki} = \Lambda_{ki}Y_{ki}^T\left(\frac{1}{\alpha}\left(\dot{x}_i - \dot{\hat{x}}_i\right) + 2\left(x_i - \hat{x}_i\right)\right) \quad (24)$$

$$\dot{\hat{\vartheta}}_{di} = -\Lambda_{di}Y_{di}^T s_i,$$

where $K_{\mu i}$ satisfies $\lambda_{\min}\left(K_{\mu i}\right) \geq \sup_{t\geq 0}\|\mu_i\,(t)\|$, and estimators $\hat{x}_i$, $\dot{\hat{x}}_i$, $\ddot{\hat{x}}_i$ are derived from

$$\dot{\hat{x}}_i = -\beta_1\mathrm{sgn}\left(\sum_{j=1}^{m}\omega_{ij}(\hat{x}_i - \hat{x}_j - \delta_i + \delta_j)\right. $$

$$\left. + b_i(\hat{x}_i - \delta_i - x_0)\right),$$

$$\ddot{\hat{x}}_i = -\beta_2\mathrm{sgn}\left(\sum_{j=1}^{m}\omega_{ij}(\dot{\hat{x}}_i - \dot{\hat{x}}_j) + b_i(\dot{\hat{x}}_i - \dot{x}_0)\right),$$

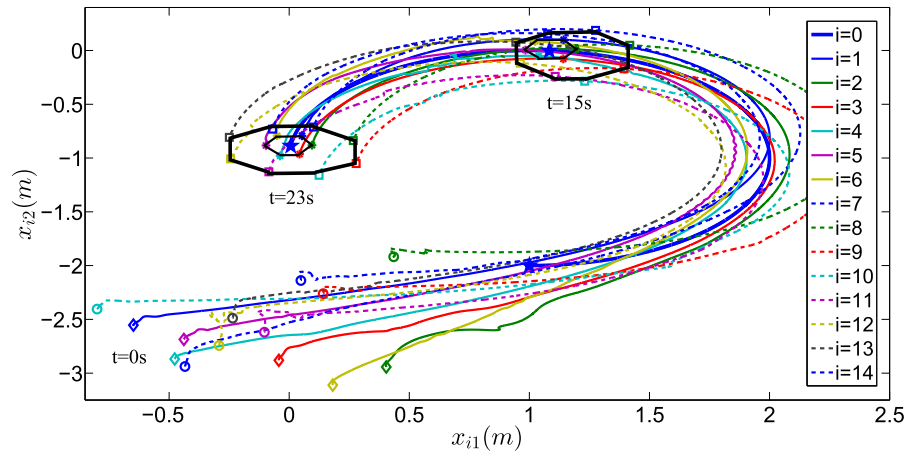**Fig. 13** The task-space formation tracking performance of case (**c**)

Fig. 14 The task-space position tracking errors $\tilde{x}_i$ of the robots under control algorithm (24)
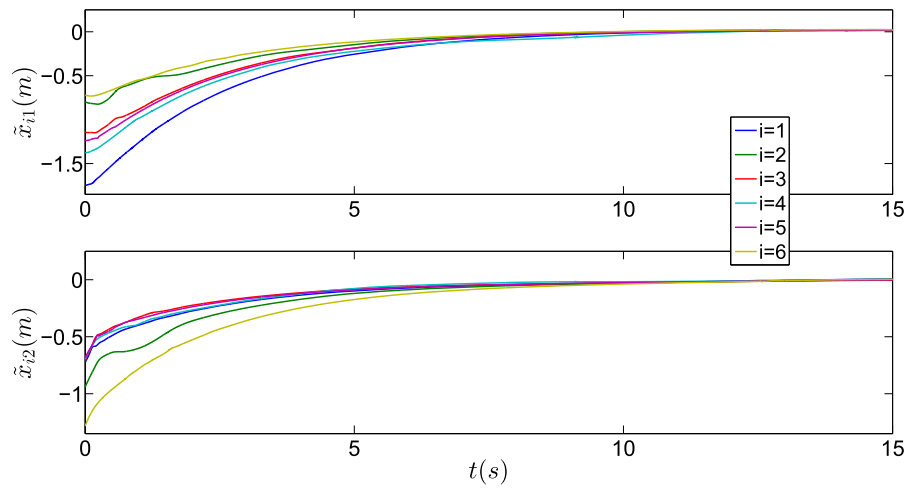

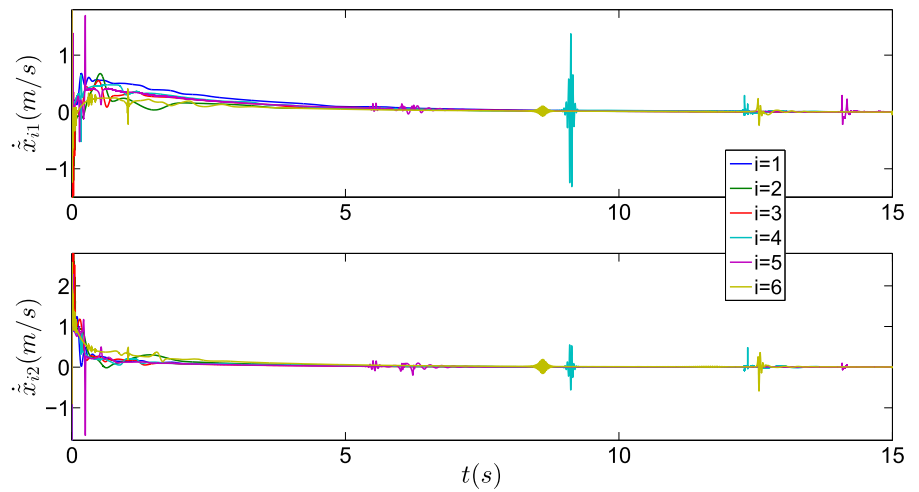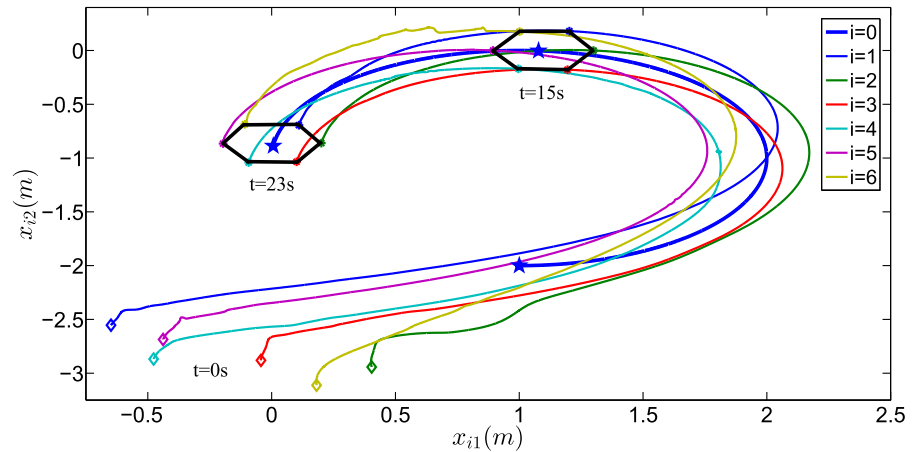**Fig. 15** The task-space velocity tracking errors $\dot{\tilde{x}}_i$ of the robots under control algorithm (24)

Fig. 16 The task-space formation tracking performance under control algorithm (24)

$$\dddot{x}_i = -\beta_3 \text{sgn}\left(\sum_{j=1}^{m} \omega_{ij}(\ddot{\tilde{x}}_i - \ddot{\tilde{x}}_j) + b_i(\ddot{\tilde{x}}_i - \ddot{x}_0)\right),$$
(25)

where the three proper constants $\beta_1, \beta_2, \beta_3$ satisfy $\beta_1 > ||\dot{x}_0||, \beta_2 > ||\ddot{x}_0||, \beta_3 > ||\dddot{x}_0||$.

Set $\beta_1 = 10, \beta_2 = 5, \beta_3 = 2, \lambda_{\min}(K_{\mu i}) \geq 6$, and other parameters are designed with the same as that in Example 1. Then, selecting the desired configurations as case (a), *i.e.*, every $\gamma_j = \frac{1}{6}$, the comparison results under control algorithm (24) are given in Figs. 14, 15 and 16, which show that the formation tracking problem in case (a) is finally achieved within $t = 23$ seconds. However, it is necessary to point out that Figs. 14, 15 and 16 are obtained under a single leader, which may restrict its applications, from the physical and engineering point of view, in the cases with the only single leader being disabled. Furthermore, the results are limited by the assumption that the supremum of the reference parameters $\dot{x}_0, \ddot{x}_0, \dddot{x}_0$ and the external disturbances μ_i are globally known to all robots, while, by utilizing fully distributed control algorithms and multiple leaders, Figs. 5, 6 and 7 are well obtained and are independent of parameter supremum and leader failure.

5 Conclusion

This paper has constructed several novel fully distributed control algorithms to realize the task-space formation tracking of NHRS with both single and multiple time-varying leaders. First, the nonlinear system is modeled with external disturbances, kinematic and dynamic uncertainties. Then, the main results of the system are obtained by adopting the fully distributed control algorithms, including distributed estimators and gain adaption laws, control inputs, disturbance observer, kinematic and dynamic parameter adaption laws. Next, the asymptotic stability of the obtained results is analyzed by invoking Barbalat's lemma and input-to-state stability theory. Moreover, the obtained results have been further extended to formation-containment and consensus problems with dynamical topologies. Finally, by designing corresponding control gains and parameters, numerous examples have been, respectively, performed for NHRS to verify the validity and advantages of the theoretical results. In future works, the formation tracking of NHRS with time-varying delays and external forces will be further discussed.

Compliance with ethical standards

Conflict of interest The authors declare that there is no conflict of interest.

Appendix

Appendix A. Proof of Lemma 1. By Assumption 2, it is clear that L_3 is invertible. Based on the definition of Laplacian matrix $\mathcal{L}$, one obtains $L_2 1_m + L_3 1_{n-m} = 0_m,$

i.e., $-L_3^{-1}L_2 1_m = 1_{n-m}$ since L_3 is invertible. Thus, it gives that $-L_3^{-1}L_2$ is nonnegative, and each row sums equal to one.

Appendix B. Proof of Theorem 1. Here we prove the theorem by contradiction. First we replace β_i in (11a) with a constant $\bar{\beta}_i$, which satisfies $\bar{\beta}_i > \mathcal{L}_\infty \|\dot{x}_0\|$. Then, by similar proofs of Theorem 3.1 given in [3] and Lemma 3 given in [10], one can easily obtain $x_i - x_0 = 0$ in finite time. If we assume that $x_i - x_0 = 0$ cannot be achieved in finite time such that it gives

$$\beta_i(t) < \bar{\beta}_i, \tag{26}$$

While $\dot{\beta}_i$ in (11b) satisfies $\dot{\beta}_i \geq 0$, which reveals that β_i continuously increases such that there must exist a finite time satisfying

$$\beta_i(t_1) > \bar{\beta}_i, \tag{27}$$

By comparing with (26) and (27), it is contradictory such that it follows that $x_i - x_0 = 0$ can be obtained in finite time, and it ends the proof.

Appendix C1. The details derivative of $V_{1i}(t)$. Differentiating (16) with respect to time yields

$$\dot{V}_{1i}(t) = \frac{1}{2}s_i^T \dot{H}_i(q_i)s_i + s_i^T H_i(q_i)\dot{s}_i + \tilde{\vartheta}_{di}^T \Lambda_{di}^{-1} \dot{\tilde{\vartheta}}_{di} + \tilde{\mu}_i^T \Lambda_{\mu i}^{-1} \dot{\tilde{\mu}}_i,$$

Then, by invoking (15), Properties 2 and 4, one obtains

$$\begin{aligned}
\dot{V}_{1i}(t) &= \frac{1}{2}s_i^T \dot{H}_i(q_i)s_i + s_i^T \Big(-C_i(q_i, \dot{q}_i)s_i \\
&\quad -K_i s_i - Y_{di}\tilde{\vartheta}_{di} + \tilde{\mu}_i \Big) \\
&\quad + \tilde{\vartheta}_{di}^T \Lambda_{di}^{-1} \Lambda_{di} Y_{di}^T s_i - \tilde{\mu}_i^T \Lambda_{\mu i}^{-1} \Lambda_{\mu i} s_i \\
&= \frac{1}{2}s_i^T \big(\dot{H}_i(q_i) - 2C_i(q_i, \dot{q}_i) \big)s_i - s_i^T K_i s_i \\
&\quad -s_i^T Y_{di}\tilde{\vartheta}_{di} + s_i^T \tilde{\mu}_i + \tilde{\vartheta}_{di}^T Y_{di}^T s_i - \tilde{\mu}_i^T s_i \\
&= -s_i^T K_i s_i \leq 0,
\end{aligned}$$

Appendix C2. The details derivative of $V_{2i}(t)$. Firstly, differentiating (17) with respect to time yields

$$\dot{V}_{2i}(t) = \tilde{x}_i^T \dot{\tilde{x}}_i + \tilde{\vartheta}_{ki}^T \Lambda_{ki}^{-1} \dot{\tilde{\vartheta}}_{ki} - \frac{1}{\alpha_1}(J_i s_i)^T J_i s_i,$$

Then, substituting $J_i s_i = \dot{\tilde{x}}_i + \alpha_1 \tilde{x}_i - Y_{ki}\tilde{\vartheta}_{ki}$ derived from (13a), and $\dot{\tilde{\vartheta}}_{ki} = -\Lambda_{ki} Y_{ki}^T(\frac{1}{\alpha_1}\dot{\tilde{x}}_i + 2\tilde{x}_i)$ yields

$$\begin{aligned}
\dot{V}_{2i}(t) &= -\frac{1}{2\alpha_1}\left(\dot{\tilde{x}}_i + \alpha_1 \tilde{x}_i \right)^T \left(\dot{\tilde{x}}_i + \alpha_1 \tilde{x}_i \right) - \frac{\alpha_1}{2}\tilde{x}_i^T \tilde{x}_i \\
&\quad -\frac{1}{2\alpha_1}\dot{\tilde{x}}_i^T \dot{\tilde{x}}_i - \frac{1}{\alpha_1}(Y_{ki}\tilde{\vartheta}_{ki})^T Y_{ki}\tilde{\vartheta}_{ki} \\
&\quad -\frac{1}{\alpha_1}\tilde{\vartheta}_{ki}^T Y_{ki}^T \dot{\tilde{x}}_i,
\end{aligned}$$

Based on the standard basic inequalities, one obtains $-\frac{1}{\alpha_1}\tilde{\vartheta}_{ki}^T Y_{ki}^T \dot{\tilde{x}}_i \leq \frac{1}{2\alpha_1}\dot{\tilde{x}}_i^T \dot{\tilde{x}}_i + \frac{1}{2\alpha_1}(Y_{ki}\tilde{\vartheta}_{ki})^T Y_{ki}\tilde{\vartheta}_{ki}$ such that

$$\begin{aligned}
\dot{V}_{2i}(t) &\leq -\frac{1}{2\alpha_1}\left(\dot{\tilde{x}}_i + \alpha_1 \tilde{x}_i \right)^T \left(\dot{\tilde{x}}_i + \alpha_1 \tilde{x}_i \right) - \frac{\alpha_1}{2}\tilde{x}_i^T \tilde{x}_i \\
&\quad -\frac{1}{2\alpha_1}\dot{\tilde{x}}_i^T \dot{\tilde{x}}_i - \frac{1}{\alpha_1}(Y_{ki}\tilde{\vartheta}_{ki})^T Y_{ki}\tilde{\vartheta}_{ki} \\
&\quad +\frac{1}{2\alpha_1}\dot{\tilde{x}}_i^T \dot{\tilde{x}}_i + \frac{1}{2\alpha_1}(Y_{ki}\tilde{\vartheta}_{ki})^T Y_{ki}\tilde{\vartheta}_{ki} \\
&\leq -\frac{1}{2\alpha_1}\left(\dot{\tilde{x}}_i + \alpha_1 \tilde{x}_i \right)^T \left(\dot{\tilde{x}}_i + \alpha_1 \tilde{x}_i \right) \\
&\quad -\frac{\alpha_1}{2}\tilde{x}_i^T \tilde{x}_i - \frac{1}{2\alpha_1}(Y_{ki}\tilde{\vartheta}_{ki})^T Y_{ki}\tilde{\vartheta}_{ki} \leq 0,
\end{aligned}$$

References

1. Meng, Z., Anderson, B.D.O., Hirche, S.: Formation control with mismatched compasses. Automatica **69**, 232–241 (2016)
2. Meng, Z., Yang, T., Shi, G., Dimarogonas, D.V., Hong, Y., Johansson, K.H.: Targeted agreement of multiple Lagrangian systems. Automatica **84**, 109–116 (2017)
3. Cao, Y., Ren, W., Meng, Z.: Decentralized finite-time sliding mode estimators and their applications in decentralized finite-time formation tracking. Syst. Control Lett. **59**(9), 522–529 (2010)
4. Wang, L., Zeng, Z., Hu, J., Wang, X.: Controller design for global fixed-time synchronization of delayed neural networks with discontinuous activations. Neural Netw. **87**, 122–131 (2017)
5. Liu, Y., Guo, B., Park, J.H., Lee, S.M.: Nonfragile exponential synchronization of delayed complex dynamical networks with memory sampled-data control. IEEE Trans. Neural Netw. Learn. Syst. **29**(1), 118–128 (2018)
6. Liu, Y., Guo, B., Park, J.H., Lee, S.M.: Event-based reliable dissipative filtering for T–S fuzzy systems with asynchronous constraints. IEEE Trans. Fuzzy Syst. **26**(4), 2089–2098 (2018)
7. Liu, Y., Fang, F., Park, J.H.: Decentralized dissipative filtering for delayed nonlinear interconnected systems based on T–S fuzzy model. IEEE Trans. Fuzzy Syst. (2018). https://doi.org/10.1109/TFUZZ.2018.2870079
8. Wang, Y., Liu, X., Xiao, J., Shen, Y.: Output formation-containment of interacted heterogeneous linear systems by distributed hybrid active control. Automatica **93**, 26–32 (2018)
9. Ge, M., Guan, Z., Hu, B., He, D., Liao, R.: Distributed controller–estimator for target tracking of networked robotic systems under sampled interaction. Automatica **69**, 410–417 (2016)
10. Yao, X., Ding, H., Ge, M.: Task-space tracking control of multi-robot systems with disturbances and uncertainties rejection capability. Nonlinear Dyn. **92**(4), 1649–1664 (2018)
11. Yao, X., Ding, H., Ge, M.: Formation-containment control for multi-robot systems with two-layer leaders via hierarchi-

cal controller–estimator algorithms. J. Frankl. Inst. **355**(12), 5272–5290 (2018)

12. Baranithaa, R., Rakkiyappana, R., Mohajerpoor, R., Al-Wais, S.: Stability analysis of nonlinear telerobotic systems with time-varying communication channel delays using general integral inequalities. Inf. Sci. **465**, 353–372 (2018)

13. Al-Wais, S., Mohajerpoor, R., Shanmugam, L., Abdi, H., Nahavandi, S.: Improved delay-dependent stability criteria for telerobotic systems with time-varying delays. IEEE Trans. Syst. Man Cybern. Syst. (2017). https://doi.org/10.1109/TSMC.2017.2706218

14. Mohajerpoor, R., Sharifi, I., Talebi, H.A., Rezaei, S.M.: Adaptive bilateral teleoperation of an unknown object handled by multiple robots under unknown communication delay. In: Proceedings of the IEEE/ASME International Conference on Advanced Intelligent Mechatronics, pp. 1158-1163 (2013)

15. Yu, X., Liu, L., Feng, G.: Distributed circular formation control of nonholonomic vehicles without direct distance measurements. IEEE Trans. Autom. Control **63**(8), 2730–2737 (2018)

16. Yu, J., Ji, J., Miao, Z., Zhou, J.: Adaptive formation control of networked Lagrangian systems with a moving leader. Nonlinear Dyn. **90**(4), 2755–2766 (2017)

17. Yuan, C., Licht, S., He, H.: Formation learning control of multiple autonomous underwater vehicles with heterogeneous nonlinear uncertain dynamics. IEEE Trans. Cybern. **48**(10), 2920–2934 (2017)

18. Yuan, C., He, H., Wang, C.: Cooperative deterministic learning-based formation control for a group of nonlinear uncertain mechanical systems. IEEE Trans. Ind. Inf. (2018). https://doi.org/10.1109/TII.2018.2792455

19. Dong, X., Hu, G.: Time-varying formation tracking for linear multi-agent systems with multiple leaders. IEEE Trans. Autom. Control **62**(7), 3658–3664 (2017)

20. Yu, J., Dong, X., Li, Q., Ren, Z.: Practical time-varying formation tracking for second-order nonlinear multiagent systems with multiple leaders using adaptive neural networks. IEEE Trans. Neural Netw. Learn. Syst. (2018). https://doi.org/10.1109/TNNLS.2018.2817880

21. Yu, J., Dong, X., Liang, Z., Li, Q., Ren, Z.: Practical time-varying formation tracking for high-order nonlinear multiagent systems with multiple leaders based on the distributed disturbance observer. Int. J. Robust. Nonlinear Control **28**(9), 3258–3272 (2018)

22. Li, Z., Wen, G., Duan, Z., Ren, W.: Designing fully distributed consensus protocols for linear multi-agent systems with directed graphs. IEEE Trans. Autom. Control **60**(4), 1152–1157 (2015)

23. Xu, X., Li, Z., Gao, L.: Distributed adaptive tracking control for multi-agent systems with uncertain dynamics. Nonlinear Dyn. **90**(4), 2729–2744 (2017)

24. Wen, G., Yu, W., Chen, M.Z.Q., Yu, X., Chen, G.: Pinning a complex network to follow a target system with predesigned control inputs. IEEE Trans. Syst. Man Cybern. Syst. **99**, 1–12 (2018)

25. Ding, Z.: Distributed adaptive consensus output regulation of network-connected heterogeneous unknown linear systems on directed graphs. IEEE Trans. Autom. Control **62**(9), 4683–4690 (2017)

26. Li, Z., Ding, Z., Sun, J., Li, Z.: Distributed adaptive convex optimization on directed graphs via continuous-time algorithms. IEEE Trans. Autom. Control **63**(5), 1434–1441 (2018)

27. Li, C., Yu, X., Huang, T., He, X.: Distributed optimal consensus over resource allocation network and its application to dynamical economic dispatch. IEEE Trans. Neural Netw. Learn. Syst. **29**(6), 2407–2418 (2018)

28. Spong, M.W., Hutchinson, S., Vidyasagar, M.: Robot Modeling and Control. Wiley, New York (2006)

29. Slotine, J.-J.E., Li, W.: Applied Nonlinear Control. Prentice Hall, Englewood Cliffs, NJ (1991)

30. Ren, W., Cao, Y.: Distributed Coordination of Multi-agent Networks. Springer, London (2011)

31. Liu, Z., Guan, Z., Shen, X., Feng, G.: Consensus of multi-agent networks with aperiodic sampled communication via impulsive algorithms using position-only measurements. IEEE Trans. Autom. Control **57**(10), 2639–2643 (2012)

32. Liu, Z., Yu, X., Guan, Z., Hu, B., Li, C.: Pulse-modulated intermittent control in consensus of multiagent systems. IEEE Trans. Syst. Man Cybern. Syst. **47**(5), 783–793 (2017)

33. Lozano, R., Brogliato, B., Egeland, O., Maschke, B.: Dissipative Systems Analysis and Control: Theory and Applications. Springer, London (2000)

34. Khalil, H.K., Grizzle, J.W.: Nonlinear Systems. Prentice Hall, Englewood Cliffs, NJ (1996)